



University of Liege

Academic year 2018-2019

APRI0007: Major project in electronics Final report



THE PROJECT(OR)

BLISTEIN François DRAGOZIS Romane EL OSROUTI Mohamed
LEJEUNE Gary SPITS Martin VERSLUYS Kevin

MASTER 1 - Electrical engineering

Table of Contents

1	Introduction	1
1.1	Description of the project	1
1.2	Description of the system	1
1.3	Constraints	2
1.4	Applications	3
1.5	Implementation of the project	3
2	Project management	4
2.1	Project Charter	4
2.2	Project objectives	4
2.3	Acceptance criteria	5
2.4	Project planning	5
2.5	Risks	6
2.6	Encountered problems	7
2.7	Project costs	8
3	Embedded part	9
3.1	General concept and introduction	9
3.2	Software architecture	9
3.3	Actuators and sensors	10
3.4	Implementation	11
3.4.1	Feedback of the buck converter	12
3.4.2	Measurement of distances	13
3.4.3	Control of the motor	14
3.5	Pseudo-Code	14
3.6	Assembly of the whole device	17
4	Power part	18
4.1	Choice of topology and first circuit simulations	18
4.1.1	Conception of the buck converter	18
4.2	Open-loop simulation	18
4.2.1	Voltage and current simulations	18
4.2.2	Simulations	20
4.2.3	Theoretical signals in the circuit	21
4.2.4	Measured signals in the circuit	22
4.3	Feedback loop design	23
4.3.1	Simulations	27
4.4	Closed-loop operation measurements	29
5	Linear control systems part	30
5.1	Motivation and control problem	30
5.1.1	Topic : Automatic tracking spotlight system	30
5.1.2	Description of the control problem	30
5.2	Open Loop System	31
5.2.1	Schematic of the problem	31
5.2.2	State-space representation	32

5.2.3	Simulations of the open loop system	33
5.2.4	Controllability	33
5.2.5	Observability	33
5.3	Frequency domain	33
5.3.1	Transfer function	33
5.3.2	Constraints and design considerations	34
5.3.3	Loop shaping	35
5.3.4	Final controller	44
5.3.5	Noise	45
5.4	Implementation of the controller	47
5.4.1	PID controller	47
5.4.2	Implementation of the controller	49
5.4.3	Conclusion	49
6	Mechanics and hardware	50
6.1	Motor shaft, angular sensor and ultrasound sensor	50
6.2	PCB design	52
6.3	Orientation of the ultrasonic sensors	53
7	Improvements	55
8	Conclusion	55
9	Appendix	56
9.1	Project planning	56
9.2	Risk management	57
9.3	Linear control systems part : Gang of "2"	58

1 Introduction

1.1 Description of the project

Projectors are devices that can be found in lots of application in the everyday life : for illuminating singers during a concert, humorists during their show and so on. The idea of this project is based on these applications and the goal is to build and implement a movable spotlight that will track someone moving in a room and light him during its movement.

From a practical point of view several components will be used in order to build the projector. First in order to know the location of the moving person the projector will be helped by two ultrasonic sensors. Then a DC motor located between the two sensors will make the projector move. Finally a microcontroller will be used in order to control the DC motor, and thus the direction of the projector, and its power supply. The goal of the microcontroller is thus to ensure that both distances are the same in order to track the moving body.

1.2 Description of the system

The system will consist of the spotlight and its support and the reference will be the moving person in the room. The microcontroller will compute and control the angular position at which the spotlight should be in order to light the tracked body. It will thus take as input the position of the moving person and depending on that the DC motor torque will change in order to make the system move in a certain direction. The information of the location of the moving person will come from the two ultrasonic emitter-receiver sensors. The block diagram which illustrates the links between all the components of the system is represented in FIGURE 1.

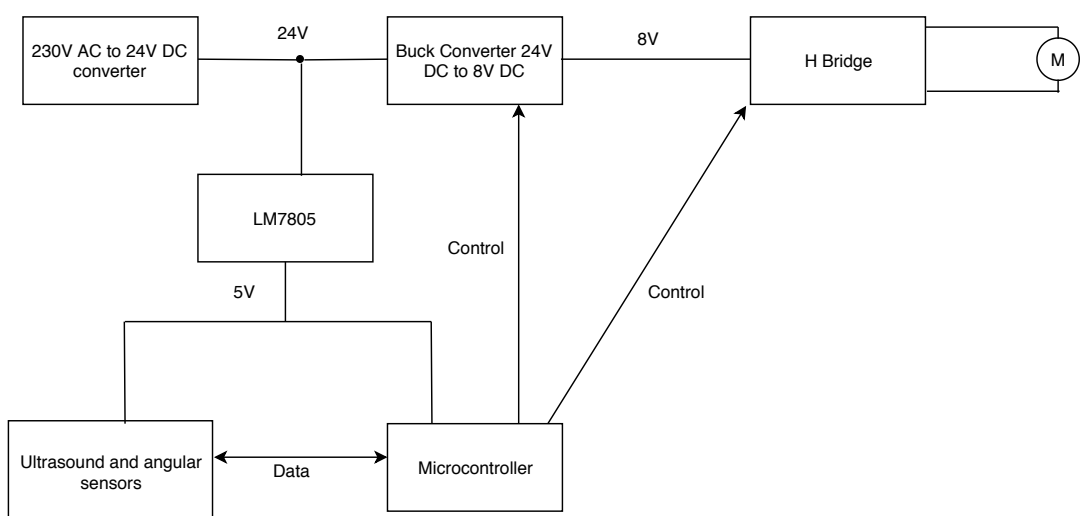


Figure 1: Block diagram of the whole system

In fact a AC-DC converter from $230V_{AC}$ to $24V_{DC}$ ¹ will supply the DC-DC buck converter from $24V_{DC}$ to $8V_{DC}$ and the voltage regulator LM7805. Then the buck converter that will be entirely build and implemented will supply the H-bridge which will drive the motor. The two ultrasonic sensors will compute the distance between them and the moving body and the microcontroller will control the buck converter and control the DC motor in order to track the moving person thanks to the data sent by the ultrasonic sensors.

1.3 Constraints

The system will be inevitably subjected to some constraints that will be taken into account during the whole design of the project. Here is the list of these constraints :

- Each ultrasound emitter-receiver sensor is limited by a maximum range in which the distance can be computed and its directivity. This limitation is represented in FIGURE 2 ;
- The speed of the moving human body will be limited such as the system has enough time to respond ;
- The person must be alone in the room.

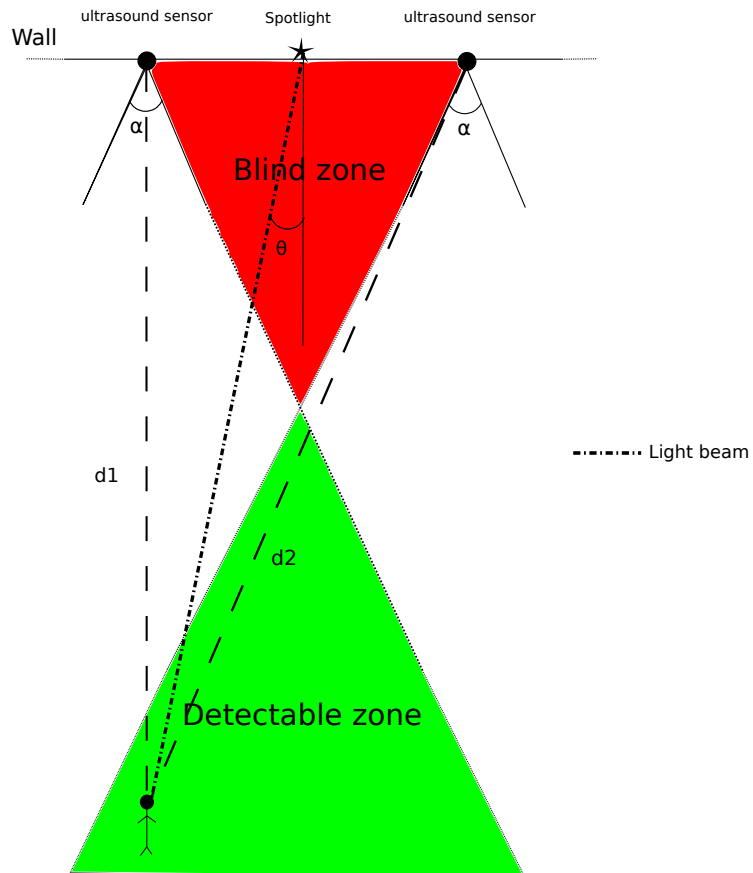


Figure 2: Limitation of the maximum range of the sensor

¹In practice the voltage supply from the laboratory will be used since the DC-DC converter could not be bought.

1.4 Applications

Some applications can be developed based on the implemented project. Here is a list of some examples of these potential applications :

- *Security system* : automatic motion tracking and lighting intruders in a property or of prisoners escaping from a jail ;
- *Scene lighting system* : automatic motion tracking and lighting of people on stage ;
- *Video* : the support could be used for a camera instead of a spotlight for automatic tracking of people to film.

1.5 Implementation of the project

This report is divided in several parts. Each one focuses on the different part of the whole system implementation.

First of all the management part is introduced. In this section the project objectives has been described as well as the constraints of the implementation. Also the risks that could be met or the ones that have been met have been detailed and the encountered problems as well. Finally the overall cost of this project is detailed in this first part.

Then the embedded part is developed. In this last one the hardware circuit is described as well as the software architecture of the system. Then the sensors and actuators that we have chosen to use and the interactions between the different system modules are described. Also the implementations of the buck converter feedback, the distance measurement and the motor control are detailed.

The power part is then developed. In this last one the implementation and the building of the buck converter is entirely described. Then the open-loop as well as the feedback loop design are explained and corresponding simulations are shown. Afterwards the closed-loop operation measurements obtained in practice are shown.

Then the linear control systems part is developed. This part focuses on the motivation of the controller implementation. The open loop system is then studied and then the close-loop system in the frequency domain. To finish the implementation of the controller in practice is detailed in this last section.

Finally the mechanics and hardware are described in a specific section. In this last one the components such as the actuator, the sensors and other are shown as well as the PCB design. Then the possible improvements that could be done in this project are described, the final conclusion follows this last section and close this report.

2 Project management

2.1 Project Charter

The project charter summarizes the goals that need to be achieved by our project, as well as the conditions under which the project device will operate.

Scope of the project

The system should be able to track a person in a room, such that the attached projector lights the person at all times. The tracking must be done with sufficient accuracy and speed. The person is likely to move to one direction or another, move closer to or away from the system, accelerate, decelerate, or stop.

The system must be able to keep equal distances from the person as measured by both ultrasonic sensors. The system needs to be supplied with any constant voltage between 20V and 30V, which is to be converted by a dedicated, digitally controlled circuit. Both these tasks are to be managed concurrently by the microcontroller. The power converter switching frequency must be around 30kHz.

Working conditions

- The speed of the moving object/person is limited to the human walking speed (5 km/h).
- The minimum range of the device is 0.2 meters.
- The maximum range of the device is 4 meters.
- A limited angle of detection of the ultrasonic sensors (of 15°).
- There is only maximum 1 person at a time in the operating range of the system
- Only 2D planar movement of the person is considered (in a plane parallel to the floor).
- The person must be at the same level as the system, and, if modeled, must keep reasonable proportions (i.e. not too small).

2.2 Project objectives

The goals for the project, as defined in the project charter, are summarized in Table 1.

Project objectives		Success criteria
Scope:	Tracking and lighting the person at all times	Must be able to follow the person with sufficient speed and accuracy (Detect and point to the person in less than 1 sec)
Constraints:	The system must respect all previously mentioned constraints	Device functional under the considered constraints
Time:	Deadline : 13/05/2019	Project submitted on time
Cost:	Maximum 100 €	Maximum cost not exceeded and as cheap as possible
Quality:	The device is robust and operational	The moving person is tracked and illuminated correctly

Table 1: Project objectives and success criteria.

2.3 Acceptance criteria

A summary of all global success criteria is given in Table 1. In particular, the device is considered as functional if it verifies the following:

- Accurate tracking of the moving person (tolerance of 1°).
- Sufficiently quick reacting system (follows the movement in under 1 second)

Optional improvements

The following possible improvements are considered:

- Command to reset the system to a preset position ;
- Projector turned off when nothing detected ;
- Changing the light beam width as a function of the distance between the person and the wall.

2.4 Project planning

The plan used to coordinate the execution of this project can be found in the Appendix. In this planning, the critical path (in red boxes in the chart) to follow in order to respect the imposed deadlines is defined. The planning is divided into different parts, each one in relation with a particular aspect of the project such as management, embedded systems, power electronics, linear control or hardware.

The deadlines and main steps of the project execution are displayed in Table 2, along with their due dates and the actual submission dates.

Main steps and deadlines	Due date	Actual date
Groups creation and first project definition	17-Sep-18	17-Sep-18
Presentation of proposed student project	8-Oct-18	8-Oct-18
Final definition of the project	8-Oct-18	8-Oct-18
Choice of topology and first circuit simulations	29-Oct-18	29-Oct-18
Magnetic design	19-Nov-18	19-Nov-18
Hardware and software architecture	19-Nov-18	19-Nov-18
Planning	26-Nov-18	26-Nov-18
Power converter	17-Dec-18	17-Dec-18
Sensor and actuators validation	18-Feb-19	18-Feb-19
Report on risk assessment and risk mitigation (FMEA)	18-Feb-19	18-Feb-19
Filmed project status presentation	25-Feb-19	25-Feb-19
Feedback design and simulations	4-Mar-19	4-Mar-19
Closed-loop operation measurements	1-Apr-19	8-May-19
System modules interaction check	1-Apr-19	19-Apr-19
Final report	20-May-19	20-May-19

Table 2: Project deadlines, corresponding due dates and the actual one at which each report has been sent.

FIGURE 3 shows a summary of the project progress in the form of a bar chart of due and actual submission dates.

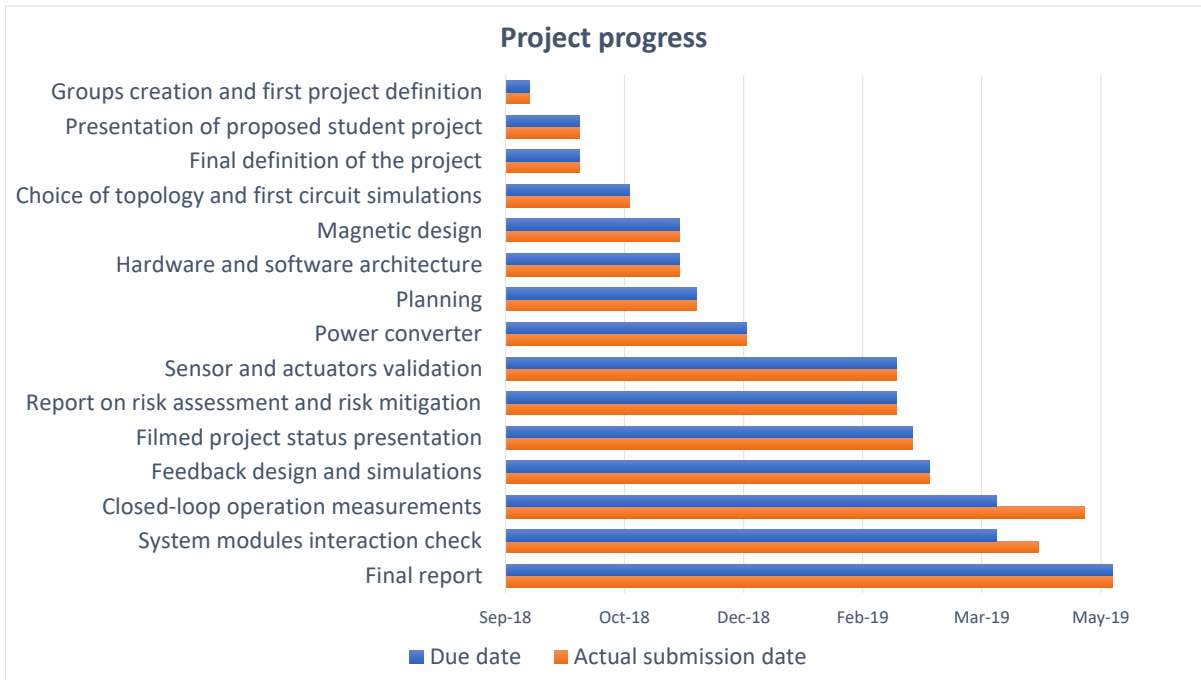


Figure 3: Predicted and actual project progress chart.

From FIGURE 3, it can be observed that the due dates were respected during the first semester, which proves the project was progressing accordingly with the planning. In between the two semesters an empty period can be distinguished, corresponding to the January examination session. During the second semester, some deadlines were completed late, due to some problems that were not anticipated earlier, or to some problems that took longer than predicted to solve (see Sections 2.5 and 2.6). Fortunately, these delays were eventually caught up at the end of the second semester, leading to the project to be submitted on time.

2.5 Risks

This section gathers the main risks and encountered problems during the realization of this project. A document with all the risks identified earlier this year, as well as their ratings and specifications, can be found in the appendix of this report (in FIGURE 64). The main risks have been listed below :

- **Ultrasound sensors.** One of the biggest risks identified from the start was the reliability and accuracy of the ultrasound sensors. Indeed, their behavior can vary hugely depending on the surface they are facing. Surfaces such as clothing can cause the sensor to give erroneous values. This is due to sound absorption and redirection of the ultrasound waves on non-smooth surfaces. This problem was partly solved by using a flat surface in front of the person for detection purposes. This allowed to have much more stable

distance measurements with the sensors. Therefore, it adds an assumption to the working conditions of the device that were established earlier.

Another possible issue was the low measuring angle of the sensors, which is of 30° , but of only 15° for more efficient measurements. This could lead to having only a small area visible to the system.

- **Simulations vs. reality.** A potential big concern for this project was to know if the practical tests would keep up with the simulations realized throughout the year. It was not guaranteed that the implementation of the linear control systems designed for the buck converter and for the projector control in assembly code on the PIC microcontroller would be possible or not.
- **Buck converter control.** Initially, we were confident in our ability to control the buck DC/DC converter using the microcontroller. The estimated risk of failure was thus low.
- **LCS implementation.** We identified early that implementing the whole linear control system design in assembly code would be a complex task. A bad implementation could result in poor tracking, vibrations, delays, etc. The risk due to an incorrect LCS implementation was thus estimated to be high, as it would be both damaging and hard to detect.

2.6 Encountered problems

The encountered problems are listed just below :

- **Error in the converter output voltage.** The buck converter open-loop output voltage is 10V instead of the predicted 8V. The load was modeled by 10 ohms, but it is actually 2 ohms.
- **Buck converter control.** In practice, contrary to what we expected, we struggled with the assembly code and it took us a lot of time to tune the closed-loop control of the converter. Especially, it was really hard for us to identify exactly where the problems came from, if it was hardware-caused or software-caused.
- **Sound interference in ultrasound sensors.** Due to sound absorption and redirection with non-smooth surfaces like clothing, the ultrasound sensors experienced some failure and interference as predicted. This problem was solved by using a flat surface to model the human body to be tracked.
- **Measuring distance of ultrasonic sensors.** Upon testing, it was noticed that the measuring distance of the sensors is actually lower than that predicted on the datasheet. This may be due to sound absorption, reflection, and also too small target. The distance also decreases with increasing angle from the axial direction of the sensor, as can be seen in FIGURE 61.
- **Low angle of detection of the ultrasound sensors.** The low angle of measurement of the sensors caused a problem of area of detection of the person. Indeed, the sensors must have a suitable orientation, which was to be determined. A solution for this particular problem is exposed in Section 6.3. The theoretical value of 30° for the orientation was later replaced with an empirical value of 20° .

2.7 Project costs

The total cost for this project is of about **55.74 €**. This amount is under the maximum project cost allowed. A summary of all different project costs is displayed in TABLE 3.

Component	Cost [€]	Note
Microcontroller	0	Provided by the Department
Ultrasonic sensors (HC-SR04)	4.8	
Angular sensor	13	
DC motor	9	
MOSFETs	4.98	
Schottky diodes	1.5	
H-bridge	4.5	
Hinges for the ultrasonic sensors	4.58	
Mechanical parts, shaft, plates, screws	5.88	Including recycled material
Headers for ultrasonic sensors	2.5	
Resistors, inductances, capacitors	0	Provided by the Department
Soldering material and cables	0	Provided by the Department
Stand for the system	0	Recycled
DC power plug	0	Recycled
Miscellaneous	5	
TOTAL COST :	55.74	Lower than max. allowed cost (100 €)

Table 3: Components needed to build the project and corresponding prices.

3 Embedded part

3.1 General concept and introduction

The block diagram of the whole system is represented in FIGURE 1.

For the power part, an AC-DC power supply will be used to get rid of a battery (no problem of discharging, charging, ...). The buck converter will have to convert $24V_{DC}$ into $8V_{DC}$ with the highest efficiency. The microcontroller will have to control the output of the buck with a feedback loop, to have a constant voltage despite a change of load.

A H-bridge will be used to control the speed and direction of rotation of the DC motor (whose shaft is connected to the spotlight). This one will be powered straightforward by the buck converter instead of the LM7805 in order to avoid losses.

The microcontroller which is supplied by the LM7805 will control the actuator and receive the data from the ultrasonic sensors.

3.2 Software architecture

A. Tasks :

1. Task τ_1 : Each $T_1 = 20$ ms, the microcontroller sends a signal to the right or left ultrasonic sensors to start measuring the distances. The execution time is $\tau_1 = 80 \mu s$. And the duration of the received pulse signal (depending of the distance) is computed and stored in ram. Very important : the measurement of the two distances cannot be done simultaneously (risk of confusion).
2. Task τ_2 : The microcontroller computes the speed of rotation of the DC motor depending on the pulse duration difference between the two sensors and control the H-bridge. So the duty cycle will be proportional to the distance difference. This task is not periodic and the execution time is negligible.
3. Task τ_3 : PID of the buck : the output voltage is sampled and new PWM being computed at at half the switching frequency : $30 \text{ kHz}/2 = 15\text{kHz}$. The total acquisition time of the analog-to-digital conversion is $15 \mu s$. The computation time of the PID is $1 \mu s$
4. Task τ_4 : Angular sensor : When a button is pushed, the angular position of the projector is computed and the system is reset to a starting angle. This task is assumed to be non periodic, and very fast.

B. Best software architecture :

From the different tasks that have to be operated by the microcontroller :

- Task 1 : $T_1 = 20$ ms, $C_2 = 80 \mu s$
- Task 2 : $T_2 : /$
- Task 3 : $T_3 = \frac{1}{15 \text{ kHz}} = 66.6 \mu s$, $C_3 = 16 \mu s$
- Task 4 : $T_4 : /$

Which software architecture is the most well suited for this application ? Ideally, it is the simplest architecture whose maximum response time (MRT) is lower than the period of the critical task. The critical task is the one with the lowest period among all tasks. In this case, it is the management of the buck converter, i.e. Task 3, with a period of $66.6\mu s$

- **Round Robin architecture :**

$$MRT = \sum_i C_i = 80\mu s + 16\mu s > 66.6\mu s$$

The Round Robin architecture is thus not suitable for this application.

- **Round Robin with interrupts :**

If task 3 is placed in the interrupt routine (because the execution time is small compared to task 1): $MRT = \sum_i C_i = 80\mu s < 20 \text{ ms} = T_1$

The Round Robin architecture with interrupt is the simplest architecture which fits our problem and it is thus the one that is chosen as software architecture.

3.3 Actuators and sensors

Here is a list of the actuators and the sensors used in the system :

- *H-Bridge : L298HN* : A double H bridge quite easy to use. (Only one of the 2 included h-bridge is used)

Purpose and the connection made on the pins :

- On input pins $IN3$ and $IN4$ are set the direction of the motor.
- On the pin EnB , the PWM which will manage the voltage across the motor is put.
- Output pin $OUT3$ and $OUT4$ are connected to the input of the DC motor.
- On pin $Sense_B$ if a resistance is connected, that will shut down the H bridge if current is too high. But in our case it is connected it to the ground to get rid of this problem.
- V_{ss} is the input logic voltage (5V in our case).
- V_s is the input voltage coming from the buck converter supplying the motor. (8V)
- GND pin is connected to the ground of the circuit.

- *Ultrasound sensor : HC-SR04* : Used to calculate the distance of an object with a ultrasound transmitter and a ultrasound receiver.

The operation is as follows: a pulse of minimum length of 10 us is sent on the pin "Trigger" of the component, then it returns a pulse length proportional to the distance measured on the pin "Echo".

CCP module of the PIC is very suitable for this application. (more explained in the implementation part)

Note : 50ms have to go before the next trigger. This is to ensure the ultrasonic wave has faded away and will not cause a false echo.

- *Angular sensor : ReYeBu Holzer angle sensor* : Very simple sensors, V_{CC} is connected to +5V and GND to 0V, and the angle can be measured just by measuring the voltage on the OUT pin. So the only thing to do is to connect the output to an analog input of the PIC.

How the implementation with all the connections with the PIC is explained in the "Implementation part" section of the report.

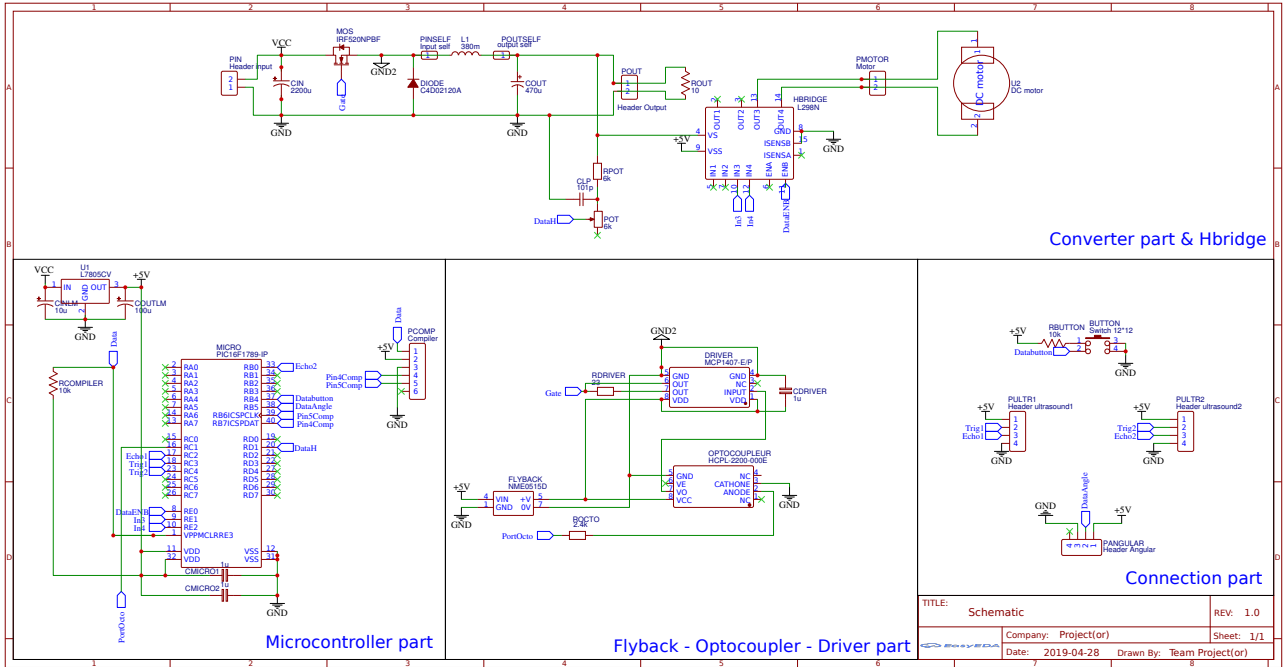


Figure 4: KiCad schematic of the whole electronics.

3.4 Implementation

In this part the implementation is explained as well as the choice of the modules used for the implementation of the PIC. The oscillation frequency is chosen equal to 32MHz and all the timers were used :

- Timer0 : Overflow of this timer (8 bits) triggers an interrupt which is used to trigger a ADC conversion to calculate the new PWM of the feedback loop of the buck.
- Timer1 : Used in the capture module (CCP1), which detects the rising and falling edges of the echo pin of the ultrasonic sensor, this timer is used to calculate the pulse time and therefore the distance measured.
- Timer2 : Used to set the PWM frequency (need to use a PWM at 30Khz frequency for constraints in the power section of the project)

2 analog pins of the PIC (Used with ADC interrupt) are used :

- RD1 (AN21) : Used for the feedback of the buck. (after a voltage divider not to burn our PIC, and a potentiometer is used for tuned our output voltage)
- RB5 (AN13) : Used for the angular sensor to know what is the angle of our projector.

Also the 3 CCP modules of the PIC are used :

- CCP1 : Used in capture mode in order to detect a rising-edge or falling-edge from echo of the ultrasound sensors. (We alternate from left to right sensor with the CCP1SEL bit of the APFCON register)

- CCP2 : Manage the duty cycle of the buck converter. This one is adjusted at 30 kHz.
- CCP3 : Manage the duty cycle of the motor's EnA pin to control its input voltage.

3.4.1 Feedback of the buck converter

As explained above, Timer0 is used to trigger an interrupt when it overflows. Timer0 is on 8 bits, our instruction frequency is $32/4 = 8$ MHz. So it triggers an interrupt every $256/8000000 = 3.2 \cdot 10^{-5}$ s which is a frequency of 31KHz. So, to have a 15kHz correction frequency of the feedback loop of the buck, a prescaler of 2 has to be put on the Timer0, which is done by setting the bits PSA and PS of the OPTION_REG to "0000".

When the interrupt of Timer0 is triggered, it triggers a conversion on pin RD1 (AN21), and this conversion will also trigger an interrupt (By setting interrupt on ADC in INTCON register) to read the value of ADC and then compute the new PWM required to apply to the MOSFET of the buck². (Computation of the new PWM to apply is explained in the power part of the report)

To summarize, the diagram in **Figure 5** shows the order of the different steps to implement the feedback loop of the buck.

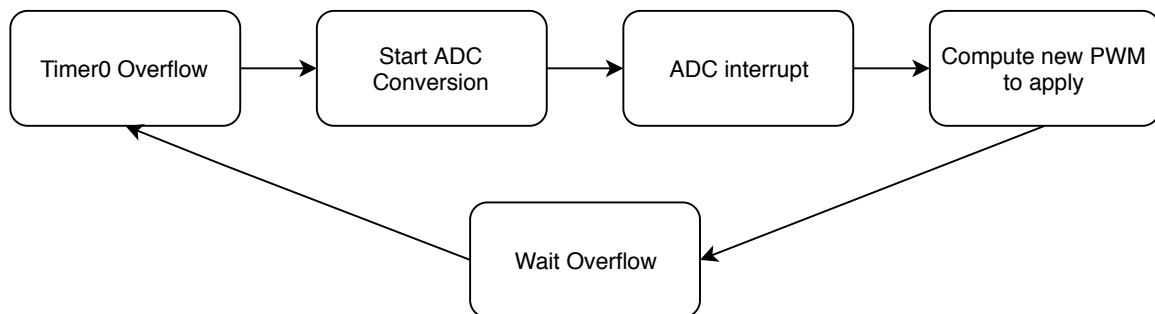


Figure 5: Different steps of the feedback loop of the buck converter.

The PWM is connected to the pin RC1 by setting the bit CCP2SEL of register APFCON1 to 0.

The PWM frequency is set by using the frequency formula given in the datasheet and is shown in **FIGURE 6**.

$$\text{PWM Period} = [(PR2) + 1] \cdot 4 \cdot TOSC \cdot \\ (\text{TMR2 Prescale Value})$$

Figure 6: Formula used to compute the PWM frequency.

² The output PWM is not directly applied to the gate of the MOSFET of the buck, it is necessary to use an optocoupler to be able to control the voltage V_{GS} of the mosfet

No prescaler is put on the Timer2, so in order to have a PWM at a frequency of 30kHz, PR2 register is set to 255. (Instead of doing that the prescaler could be increased to lower PR2, but this allows us to have the best resolution to control the duty cycle of the PWM)

Note : By setting this PWM frequency, the PWM frequency is also set on the EnA pin of the motor.

To set the duty cycle of the PWM the following that is given in the datasheet has been used and is rewritten in FIGURE 7).

$$\text{Duty Cycle Ratio} = \frac{\text{CCPRxL:CCPxCON<5:4>}}{4(\text{PR2} + 1)}$$

Figure 7: formula used to calculate the duty cycle of the PWM.

3.4.2 Measurement of distances

The ultrasonic sensors work as follows : a pulse of 10 us is sent on the trigger pins of the ultrasounds sensors (at 20 ms of interval per sensors). The CCP1 module is used in "capture mode" to capture the rising and falling edges of the echo pin, and the length of this pulse will give us the distance measured.

When a capture occurs the value of Timer1 (16 bits) is put in the register CCP1H and CCP1L. Note : It will trigger an interrupt when a capture occurs. (By setting interrupt register to the right value, etc,...)

Therefore, to measure a distance, a pulse is sent on the trigger pin. The capturing rising edge mode is thus triggered and as soon as a rising edge is captured Timer1 is turned on and initialized to 0. Then the capture mode of falling edge is triggered and when this one captures a rising edge, an interrupt which will calculate the distance according to the register CCPR1L and CCP1H (whose value of the timer 1 was copied) is triggered.

Since the best resolution for our distance was wanted, so what would be nice to have the Timer1 which is incremented to a value close to the maximum for a person at 2m50. The time corresponding is : $2.5 \cdot 2/340 = 0.0147s$. Without prescaler that corresponds to a maximum value of Timer1 of $0.0147 \cdot 8000000 = 117600$ which is too high. So only a prescaler of 2 is put on Timer1 (in register T1CON) which will lead to a maximum value of 58800 what will fit in the 16 bits of Timer1 registers.

On the other hand, since already 2 CCPs modules are used of our PIC and 2 others are needed for our 2 ultrasound sensors, this 3rd module has to be shared (because the 2 others are critical). So a very simple way is to switch from the first ultrasonic sensor to the second just by changing the bit CCP1SEL of APFCON register. (The trigger of the second sensor occurs only 25 ms after the first one, to avoid interferences between ultrasound sensors)

To summarize, the diagram in FIGURE 8 shows the different steps to implement our distance measurements.

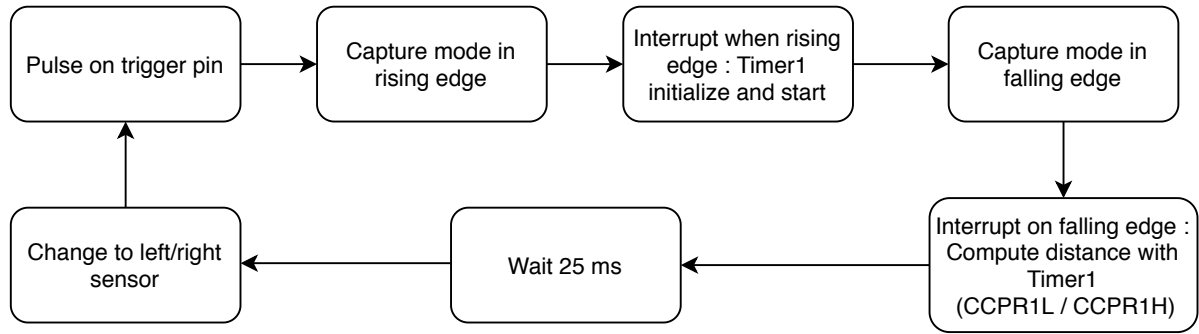


Figure 8: Different steps for the measurement of the distances.

3.4.3 Control of the motor

The idea is to track a person who is moving around the projector. Due to real-time constraints, the feedback of the motor is managed using a simple integrator term. Each 40 ms, the distances d_1 and d_2 are computed by measuring the pulse duration of each echo. As a result, the reference of our "PID" which is in fact only a "PI" controller. The error term at each discrete time step n is :

$$e[n] = d_2 - d_1$$

As said in section 5, the torque of the DC motor has to be controlled. The PWM duty cycle, $u[n]$, of the motor can be assimilated to the torque. This one is controlled at sampling period 40 ms (time interval to measure the distances of the 2 ultrasound sensors) using a "PID" control :

$$u[n] = u[n - 1] + K_i \cdot e[n] + K_p \cdot e[n],$$

where K_i and K_p are chosen respectively equal to 0.25 and 1.

$u[n]$ can become negative if $d_1 \geq d_2$. But the value of the CCPR3L must be positive. Since a H-bridge is used, the rotation sense of the motor can be handled easily by looking at the bit sign of $u[n]$. The value of the register CCPR3L will be equal to the absolute value of $u[n]$. ³

3.5 Pseudo-Code

The code is a round robin architecture as determined in section 3.2 and is available just below.

³Since $u[n]$ is a 2's complement representation, the absolute value will be only computed if $u[n] < 0$ by taking the complement of each bit and adding 1.

```

!! initialize volatile variables

void ComputeSpeed(){
    !! compute error term
    !! compute integration error term
    !! set the PWM on CCPR3L according to the expected speed
}

void( UltrasoundPulse() {
    if( Current_Sensor == 0){
        !!send pulse of 10 us on trigger pin of the first sensor and swap in capture
        mode of rising edge
        CCP1SEL = 1;
    }
    else{
        !!send pulse of 10 us on trigger pin of the second sensor and swap in capture
        mode of rising edge
        CCP1SEL = 0;
    }
}

void DirectionOfRotation(Direction){
    if( Direction == 1){
        !! turn right by setting input IN3 and IN4 of the H-bridge bridge
    }else{
        !! turn left
    }
}

void Reset() {
    // Start angle of approx 2000
    while ((Angle > 2040) || (Angle < 1960)) {
        !! low speed on motor
        if (Angle > 2040) {
            DirectionOfRotation(1);
        }
        if (Angle < 1960) {
            DirectionOfRotation(0);
        }
    }
    !! stop motor
}

void main(){
    !! initialize pins
    !! initialize ADC
    !! initialize interrupts
    !! prescaler on Timers
    !! setting PWM frequency of CCP modules
}

```

```

While(1){
    if(ButtonIsPressed){
        !! ADC conversion WITHOUT interrupt to find the Angle of the projector
        Reset();
    }else{

        delay(25ms);
        Current_Sensor = 0;
        UltrasoundPulse();

        delay(25ms);
        Current_Sensor = 1;
        UltrasoundPulse();

        ComputeSpeed();
        if(Distance1 < Distance2){
            DirectionOfRotation(1);
        }else{
            DirectionOfRotation(0);
        }
    }
}

void Interupt_Routine(){
    if(Flag Timer0 interrupt) {
        Flag Timer0 = 0;
        !! trigger ADC conversion on AN21 (buck)
    }

    if(Flag ADC interrupt) {
        Flag ADC = 0;
        !! Compute new PWM duty cycle with ADC value
    }

    if(Flag capture interrupt){
        Flag capture = 0;
        if (CaptureModeFallingEdge) {
            if (Sensor_num == 0) {
                !! compute D1 with Timer1 register
            } else {
                !! compute D2 with Timer1 register
            }
        }
        else { //capture a Rising edge
            !! initialize and activate Timer1
        }
    }
}

```

3.6 Assembly of the whole device

Figure 9 shows all parts put together. The motor (in grey on the pictures) has a unique shaft that goes all the way through. The bottom part is attached to the angular position sensor and the top part is linked to the wooden support for the ultrasonic sensors. The sensors are placed on metallic hinged supports that allow to choose the orientation of the sensors. The sensors have a measuring angle of 30° . The distance between the sensors can also be adjusted (the wooden piece being 1 meter long).

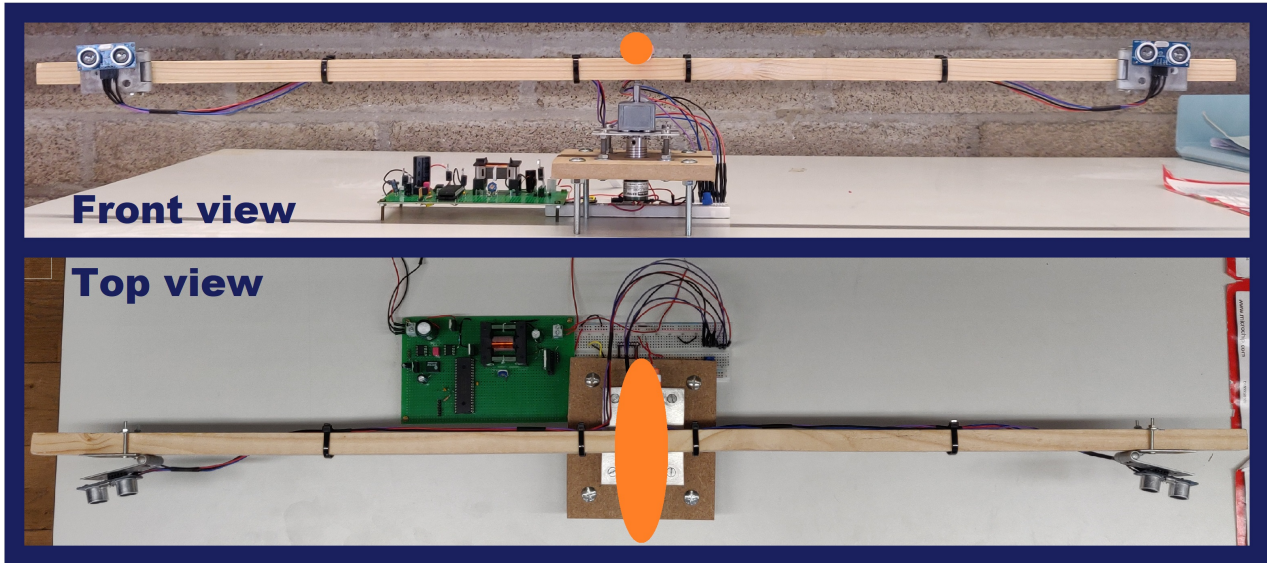


Figure 9: Entire system. The light source is not attached yet to the shaft but is represented here in orange.

4 Power part

4.1 Choice of topology and first circuit simulations

As explained in the introduction and in the embedded part, several components are used in the whole projector system. An AC/DC converter will be used in order to convert $230V_{AC}$ from the network via a plug into a DC voltage of 24V. This voltage will then supply the buck converter that will be designed in this report in order to have a DC output voltage of 8V from 24V. The LM7805 regulator will be supplied by the 8V and will convert it into a stable DC voltage of 5V, which will supply both parts of the projector : the part composed of the microcontroller and the sensors. Finally the H-Bridge will be supplied by the DC motor.

4.1.1 Conception of the buck converter

Our purpose is to design a buck converter in order to convert an input DC voltage of 24V in an output DC voltage of 8V. This converter is represented in FIGURE 10. In this last one V_1 is the input voltage, V_2 represents the switch voltage that is characterized by a duty cycle $D \in [0; 1]$ and the output voltage is the voltage drop across the resistance R_1 or the capacitance C_1 . Let us call this last one V_{out} .

4.2 Open-loop simulation

4.2.1 Voltage and current simulations

First let us consider the converter composed of ideal components and thus ignore the losses across the inductance L_1 , i.e. the resistance R_2 .

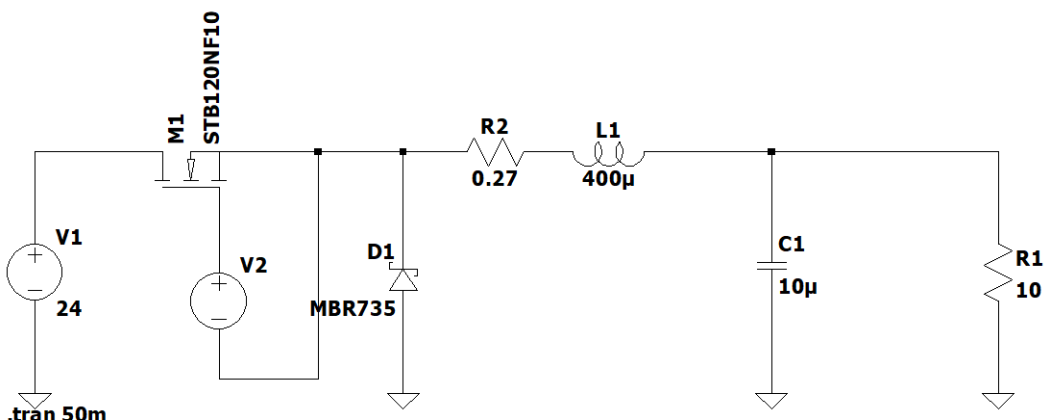


Figure 10: Buck converter schematic.

The following equation of the buck converter gives the relation between the input voltage and the output voltage :

$$V_{out} = DV_1 \Leftrightarrow D = \frac{V_{out}}{V_1} = \frac{8}{24} = 0.33$$

Now let us determine the components of the buck converter circuit in order to design the wanted one. The variation of the current that passes through the inductance L_1 is defined as follows :

$$\Delta i_{L_1} = \frac{V_1 - V_{out}}{2L_1} DT_s,$$

where T_s is the frequency of the switch voltage V_2 .

Our purpose is to find the value of L_1 , so let us do some assumptions. First let us consider that Δi_{L_1} is proportional to the nominal current $I_{n,DC}$ that supplies the DC motor (and the microcontroller as well as the sensors) as follows :

$$\Delta i_{L_1} = 30\% I_{n,DC},$$

where $I_{n,DC}$ is equal to 0.8A (from the datasheet of the DC motor). So the load resistance can be modeled as follows :

$$R_1 = \frac{V_{out}}{I_{n,DC}} = 10 \Omega$$

Afterwards the value of T_s has to be determined. In the project constraints it is written that the power converter switching frequency should be greater than 20 kHz and that 30 kHz is recommended. So let us take this last value. Finally it gives :

$$T_s = \frac{1}{f_s} = 33.33 \mu s$$

By this way the value of L_1 can be computed as follows :

$$L_1 = \frac{V_1 - V_{out}}{2\Delta i_{L_1}} DT_s = 370.3 \mu H \approx 380 \mu H$$

Then, by taking ΔV equal to 100 mV, the capacity C_1 can be computed :

$$C_1 = \frac{\Delta i_{L_1}}{8\Delta V} T_s = 10 \mu F$$

Also the following relation has to be checked for R_1 :

$$R_1 < \frac{2L_1}{(1 - D)T_s} = 34.2 \Omega \approx 34 \Omega$$

So the buck converter works well in the continuous conduction mode.

Afterwards, the values to build the inductor are computed. First, the resistance of the inductor taking a power loss worth 0.64 W is computed as follows :

$$R_L = \frac{P_{loss}}{I^2} = 1 \Omega$$

Then, the value of K_g can be computed such as:

$$\begin{cases} B_{max} = 0.25 \text{ T} \\ K_u = 0.5 \\ \rho = 1.724 \times 10^{-6} \Omega\text{cm} \end{cases}$$

$$K_g \geq \frac{\rho L_1^2 I_{n,DC}^2}{B_{max}^2 R_L K_u} 10^8 = 0.5098 \times 10^{-3} \text{ cm}^{-5}$$

So the core type EE12 is chosen and has the characteristic below:

$$\begin{cases} A_c = 1.09 \text{ cm}^2 \\ W_A = 0.476 \text{ cm}^2 \\ MLT = 6.6 \text{ cm} \\ l_m = 5.77 \text{ cm} \\ \text{core weight} = 32.4 \text{ g} \end{cases}$$

By means of these values, the different parameters of the inductor can be calculated:

$$\begin{aligned} l_g &= \frac{\mu_0 L_1 I_{n,DC}^2}{B_{max}^2 A_c} 10^4 = 4.48 \times 10^{-5} \text{ m} \\ A_L &= \frac{10 B_{max}^2 A_c^2}{L_1 I^2} = 3053.3 \text{ mH/1000turns} \\ n &= \frac{L_1 I_{n,DC}}{B_{max} A_c} 10^4 = 11.15 \text{ turns} \approx 12 \text{ turns} \\ A_w &\leq \frac{K_u W_A}{n} = 0.0213 \text{ cm}^2 = 21.3 \times 10^{-3} \text{ cm}^2 \end{aligned}$$

Thanks to these values, the wire with bare copper area less than or equal to A_w can be selected, which is the number 14 obtained by American Wire Gauge table.

Let us note that all calculations have been computed using the small ripple approximation. This means that the output voltage ripple is much smaller than the *DC* value of the output voltage, hence the output voltage can be approximated as follows :

$$v_{out}(t) = V_{out} + v_{ripple}(t) \approx V_{out}, \quad v_{ripple}(t) \ll V_{out}$$

4.2.2 Simulations

Simulations have been carried on with different input voltages (21V, 24V and 27V) and as it can be seen in FIGURE 11 the output voltage is almost constant. Furthermore, there is a voltage peak at the start of the simulation, but it is not a big deal because the voltage regulator LM7805 will stabilize this voltage right after the buck.

As the buck works in the continuous conduction mode, if the small ripple approximation is made the current ripple across the inductance at **steady-state** can be expressed as :

$$\Delta i = DT_s \frac{V_O - V_G}{L} = 0.46 \text{ A}$$

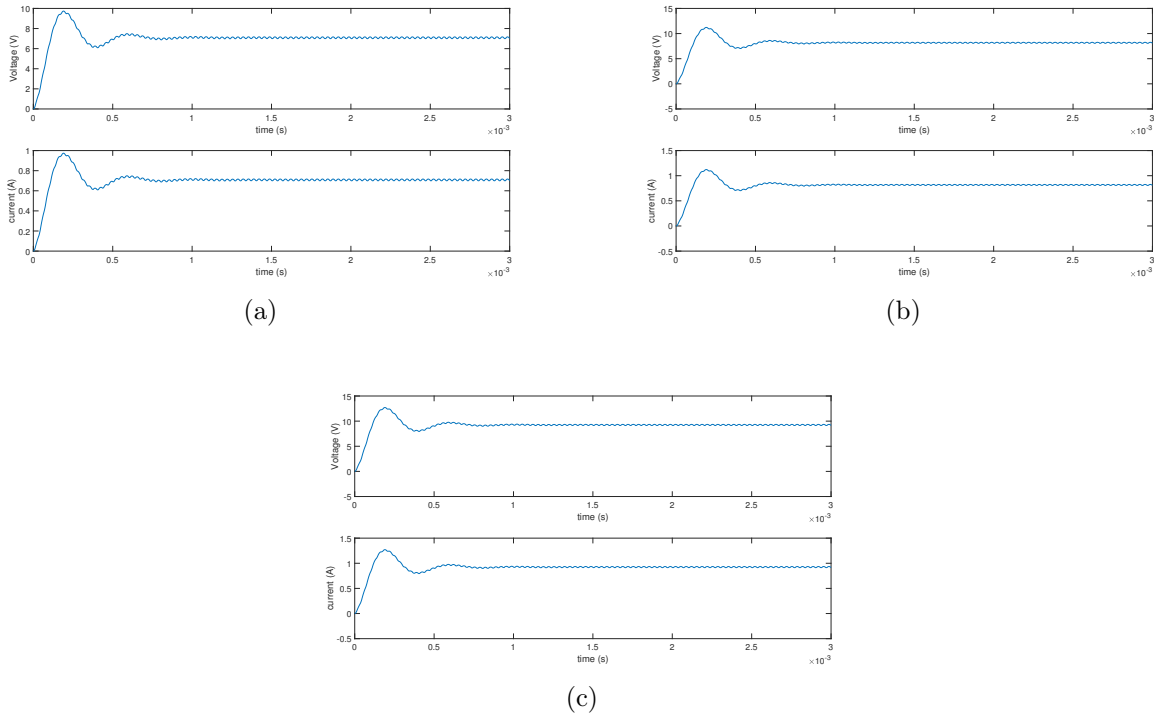


Figure 11: Simulations of the buck converter for input voltages of (a) 21V, (b) 24V and (c) 27V.

4.2.3 Theoretical signals in the circuit

The practical measurements should be as close as possible to the theoretical ones, which are represented in FIGURE 12.

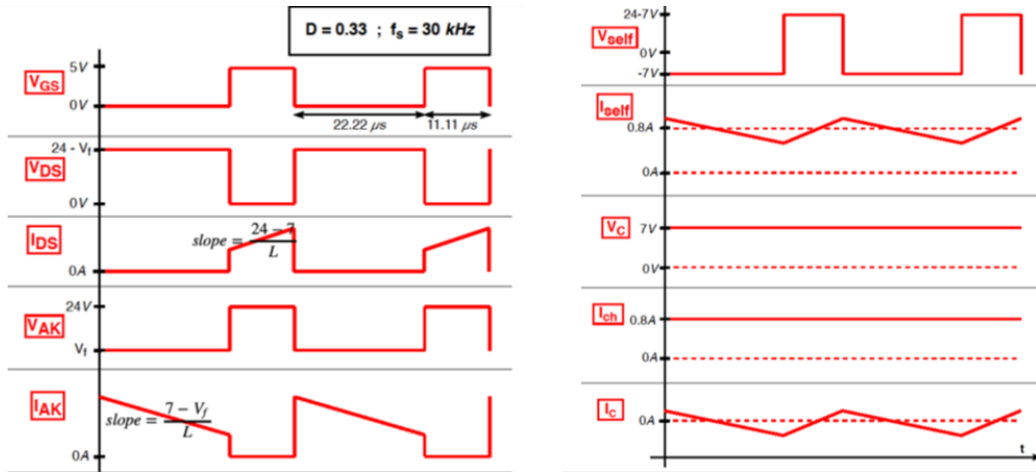


Figure 12: Theoretical signals of the buck converter.

From **LTspice** simulations, the current ripple and voltage across the inductance have the behaviour represented in FIGURE 13.

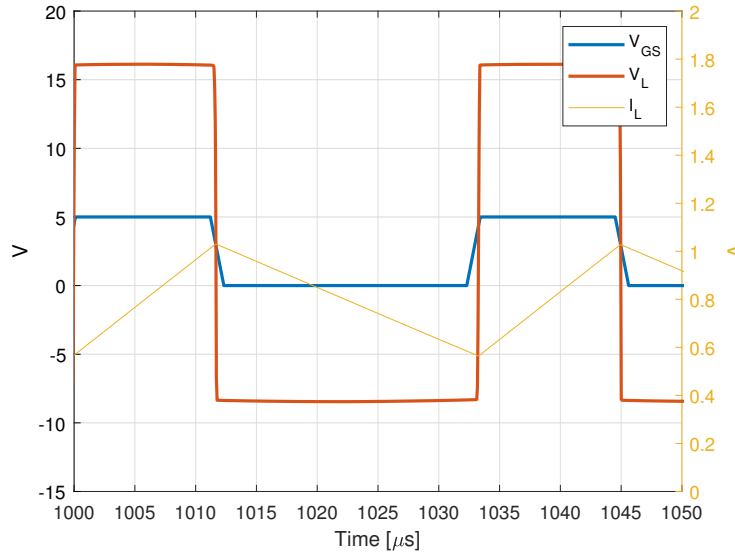


Figure 13: Simulated signals of the buck converter designed in **LTspice**.

4.2.4 Measured signals in the circuit

Then the measurements for the buck converter were made and are represented in FIGURE 14.

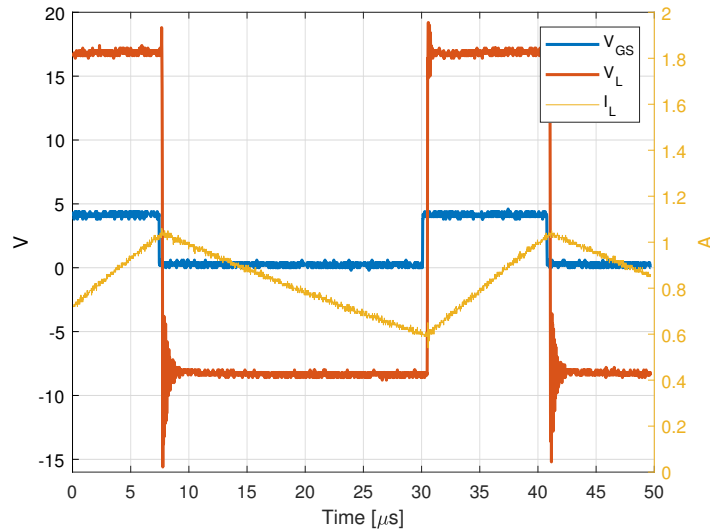


Figure 14: Measured signals of the designed buck converter.

Since the mean current is equal to 0.8A, the losses in the inductance are $P_{loss} = 0.8 * 0.27 = 0.2W$. The diode is conducting $\frac{2}{3}$ of the period, the corresponding losses must not be negligible and have to be measured. The losses in the mosfet have to be measured too.

The mean output voltage is 7V, i.e. what was expected thanks to the **LTspice** simulations. The converter works thus as expected.

4.3 Feedback loop design

The uncompensated loop transfer function of the buck converter can be expressed by the following form :

$$T_u = G_{vd}(s)H(s)G_{PWM}$$

where $G_{vd}(s)$ depends on the characteristic of the open-loop buck converter such as the inductance, the capacitor, their internal resistivity and so on. Its expression is the one as follows :

$$G_{vd}(s) = G_{vd0} \frac{1 + \frac{s}{\omega_{esr}}}{1 + \frac{s}{Q\omega_0} + \frac{s^2}{\omega_0^2}}$$

We consider a centered PWM with unity gain :

$$\tilde{G}_{PWM} = \frac{1}{V_r} \text{ with } V_r = 1$$

But we have to take into account that the modulator introduces a delay of half a switching period. Furthermore, the processing delay introduces a delay of one period so the total delay is $\tau = t_{ctrl} + \frac{T_s}{2}$. As a result, the "true" G_{PWM} is characterized by a constant magnitude of 0dB and a decreasing phase with frequency. Also we decide to work with a processing time of $T = 2 * T_s$.

In order to get rid of the high frequency interferences (harmonics of the switching frequency for example), we decided to introduce a low-pass filter with a potentiometric divider and we choose $R_1 = 1 \text{ k}\Omega$, $R_2 = 1 \text{ k}\Omega$ and $C = 1 \text{ nF}$:

$$H_a(s) = \frac{R_2}{R_1 + R_2 + R_1 R_2 C s}$$

Furthermore, due to some noise due to the quantization, a first order IIR input digital filter is often sufficient :

$$H_d(z) = \frac{a}{1 - (1 - a)z^{-1}}$$

In order to come back to the continuous domain the bilinear tustin transformation is performed in order to get $H_d(s)$. As a result $H(s) = H_a(s)H_d(s)$.

All the transfer functions described just before are represented in FIGURE 15.

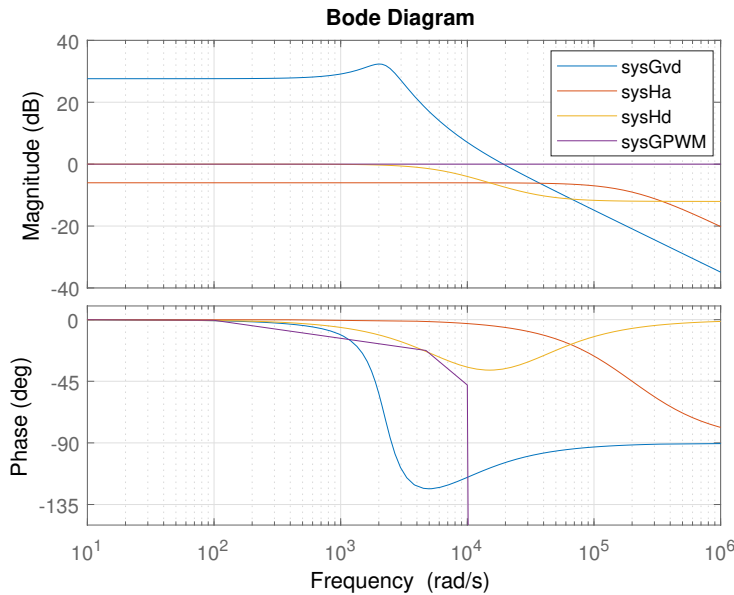


Figure 15: Bode diagrams of transfer functions : $G_{vd}(s)$, $H_a(s)$, $H_d(s)$ and G_{PWM} .

As it can be seen from the bode diagram of the uncompensated loop transfer function represented in FIGURE 16, the low frequency gain is too low so a PI controller is needed to remove the static error. Furthermore, the crossover frequency has to be adjusted and the phase margin is too small. So also a PD controller is needed in order to increase the phase margin at the neighborhood of the crossover. One good point is that the effect of the low-pass filter can clearly be seen.

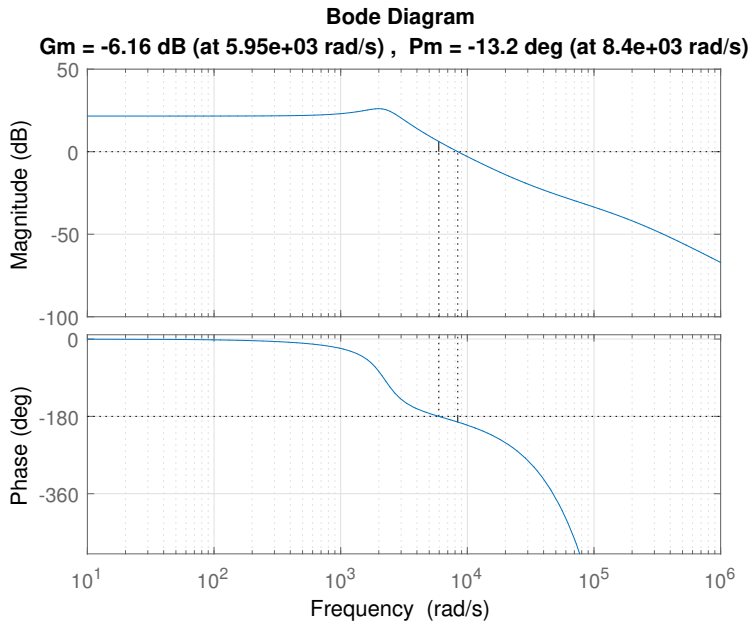


Figure 16: Bode diagram of the uncompensated loop transfer function.

The canonical form of PID controller is :

$$G_{PID}(s) = G_{PI\infty} \left(1 + \frac{\omega_{PI}}{s}\right) G_{PD0} \frac{1 + \frac{s}{\omega_{PD}}}{1 + \frac{s}{\omega_p}}$$

The values of K_p , K_i and K_d can be easily deduced from those parameters.

First, by definition, $\omega_p = \frac{2}{T} = 310^4$ rad/s. Then the crossover frequency was chosen equal to $\frac{1}{20}$ of the sampling frequency : $\omega_c = \frac{1}{20} \frac{2\pi}{T} = 4.71 \times 10^3$ rad/s. Thus it remains one degree of freedom to determine the phase margin ϕ_m :

$$\angle T(\omega_c) = \phi_m - \pi = \angle T_u(\omega_c) + \sqrt{\frac{1 + \frac{j\omega_c}{\omega_{PD}}}{1 + \frac{j\omega_c}{\omega_p}}}$$

Here the PI terms were not taken into account for simplicity reasons because the effect of the PI can be neglected around the crossover since $\omega_{PI} = \frac{\omega_{PD}}{10}$.

Coming back from the previous expression, ω_{PD} must satisfy the following expression in order to get ϕ_m as phase margin around the crossover :

$$\omega_{PD} = \frac{\omega_c}{\tan(\phi_m - \phi_u + \arctan(\frac{\omega_c}{\omega_p}))}$$

where $\phi_u = \angle T_u(\omega_c) = -170.49^\circ = -2.96$ rad.

The reason why the value of the output capacitor had to be changed from 10 μF to 500 μF was because the phase of the uncompensated loop transfer function leaded to $\omega_{PD} < 0$, $\forall \phi_m > 30^\circ$. Since the phase margin has to be above 45° in order to get a strong controller against delays, one of the intrinsic element of the buck (here the value of the capacitor) had thus to be changed. The allowed values for the phase margin with the new capacitor is : $\phi_m \leq 60$.

If a compatible phase margin for the compensated loop transfer function is fixed, ω_{PD} can be determined. Since the gain is equal to 0 dB at ω_c , G_{PD0} can be computed :

$$G_{PD0} = \frac{1}{|T_u(\omega_c)|} \frac{|1 + \frac{\omega_c}{\omega_p}|}{|1 + \frac{\omega_c}{\omega_{PD}}|}$$

where $|T_u(\omega_c)| = 24.4$ dB. $G_{PI\infty}$ is chosen equal to 1 in order to not affect the previous results. As a result, the compensated loop transfer function can be computed :

$$T(s) = T_u(s)G_{PID}(s)$$

Here are some bode diagrams of the compensated loop transfer function for different phase margins :

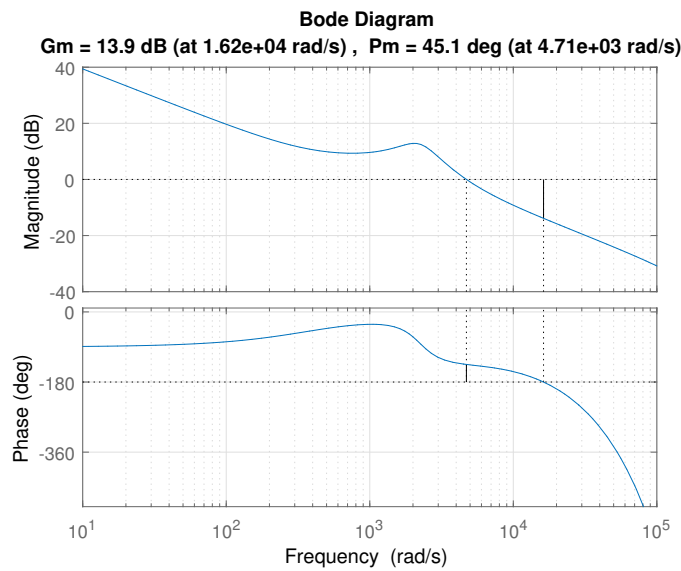


Figure 17: Bode diagram of $T(s)$ with controller characteristics : $K_p = 0.2066$, $K_d = 0.6107$, $K_i = 0.0052$.

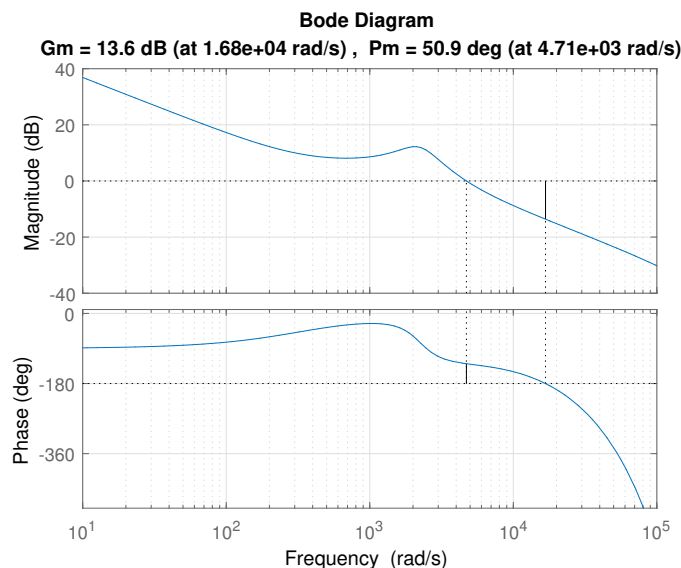


Figure 18: Bode diagram of $T(s)$ with controller characteristics : $K_p = 0.1857$, $K_d = 0.6730$, $K_i = 0.0039$.

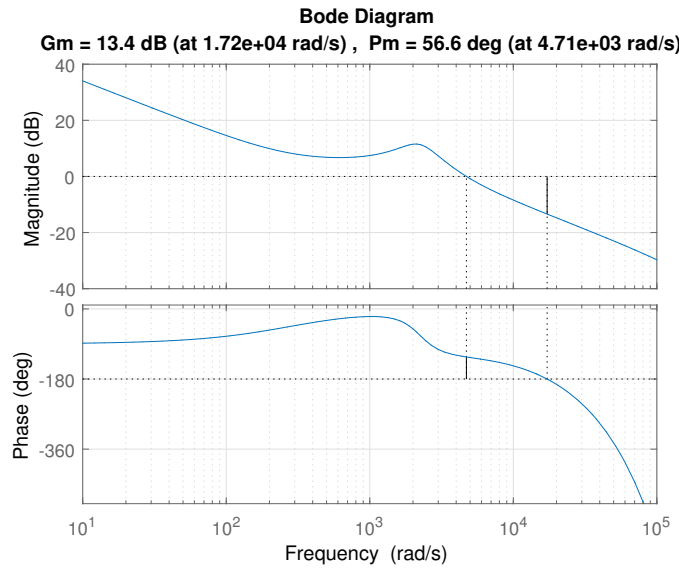


Figure 19: Bode diagram of $T(s)$ with controller characteristics : $K_p = 0.1631$, $K_d = 0.7301$, $K_i = 0.0028$.

4.3.1 Simulations

Below are the simulations of the 3 kinds of PID :

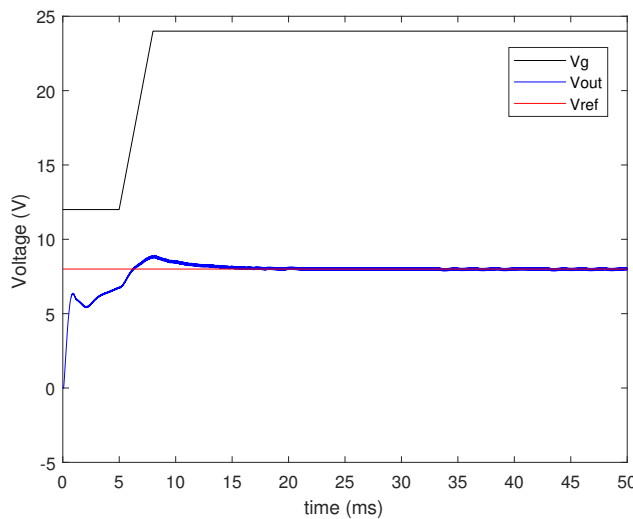


Figure 20: Simulation with controller characteristics : $K_p = 0.2066$, $K_d = 0.6107$, $K_i = 0.0052$.

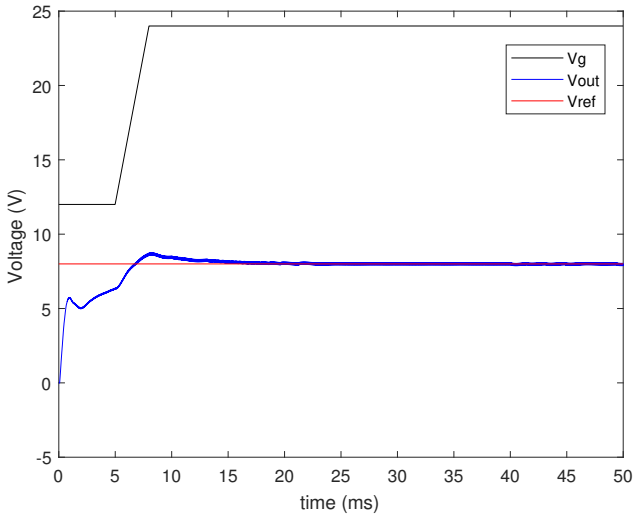


Figure 21: Simulation with controller characteristics : $K_p = 0.1857$, $K_d = 0.6730$, $K_i = 0.0039$

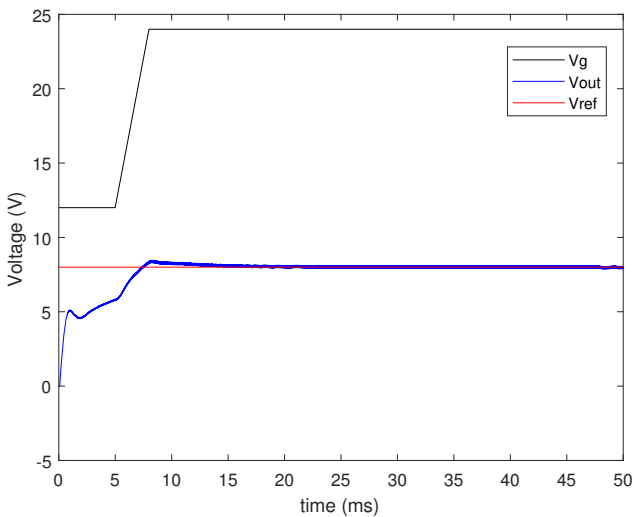


Figure 22: Simulation with controller characteristics : $K_p = 0.1631$, $K_d = 0.7301$, $K_i = 0.0028$

The graphs show that the voltage stabilizes at 8V and there is a peak of more or less 9V. By contrast, the speed at which the voltage reaches 8V changes according to the PID and it is preferable to reach this value as quickly as possible so the controller with the following characteristics is chosen : $K_p = 0.1631$, $K_d = 0.7301$, $K_i = 0.0028$.

4.4 Closed-loop operation measurements

In the previous section the parameters of the PID controller were determined (K_p , K_d and K_i), but with these values the results in practice did not give enough good measurements so these were tuned. The measurements are done by applying an input voltage AC at 100Hz sinusoidal with an amplitude higher than the output voltage expected. The best measurements are obtained with $K_p = 0$, $K_d = 0$, $K_i = 0.00488$. The measurements below are observed :

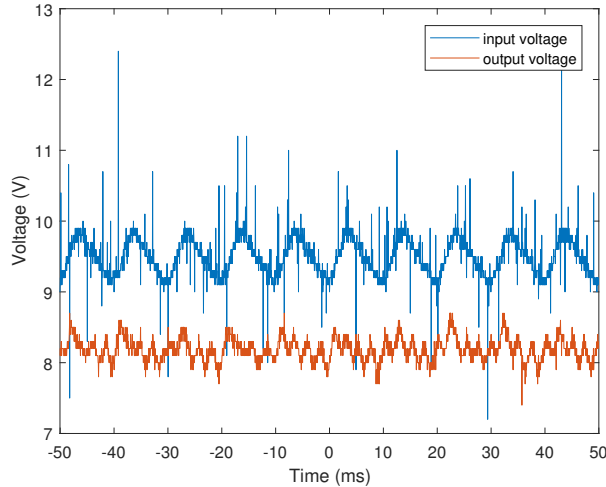


Figure 23: Input and output voltages of the buck converter in closed-loop with $K_p = 0$, $K_d = 0$, $K_i = 0.00488$.



Figure 24: Input and output voltages of the buck converter in closed-loop with $K_p = 0$, $K_d = 0$, $K_i = 0.00488$ (seen on voltmeters).

It can be seen from the graph represented in FIGURE 23 that the amplitude is greatly attenuated, the output voltage is more or less at 8V which is the expected one and the noise at 100 Hz is also attenuated. Moreover, the input DC voltage and the output DC voltage are shown in the green and the black voltmeter respectively as represented in FIGURE 24. The assembly code of the closed-loop operation can be found by clicking [here](#).

5 Linear control systems part

To design the linear control system on which our project will be based, the motivation to do so is explained as well as the control problem. Then, the open loop system is studied in detail. Finally, a thorough frequency domain analysis has been carried out in order to optimize the operation of the system.

5.1 Motivation and control problem

5.1.1 Topic : Automatic tracking spotlight system

The objective of this project is to create a light projector system that can follow a moving person in a room. In order to do that, a mobile support is used onto which are attached 2 ultrasonic sensors that compute the 2 distances d_1 and d_2 in FIGURE 25. Therefore, the sensors will allow to measure the distance between them and the person. The DC motor that allows the system to rotate is located in the middle of the support, where the projector is also located.

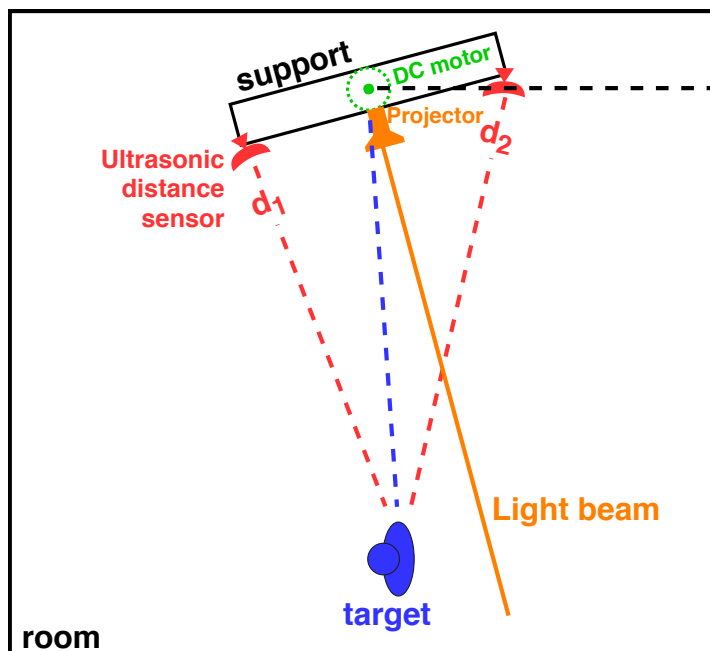


Figure 25: Diagram of the system with the projector and the target moving person.

5.1.2 Description of the control problem

The diagram illustrating the control problem is represented in FIGURE 26. The different blocks and variables used in this diagram are listed just below :

- **System to be controlled:** the system consists in the spotlight and its support.
- **Output:** the output is the angle difference between the position of the person (seen as the angle made by the person with a fixed angle origin) and the angle made by the light beam with the origin.

- **Reference:** the reference is 0. Indeed the difference between the angular position of the person (seen as the angle made by the person with a fixed angle origin) and the current angle of the motor must be equal to 0.
- **Input:** the inputs are the torque provided by the DC motor as well as the angular position of the person.
- **Sensors:** the distance sensors are some ultrasound emitter-receivers that give the distance to the closest body at each time. An angular sensor is also used to obtain the angular position of the whole system.
- **Actuator:** the DC motor drives the rotation of the spotlight and its support.

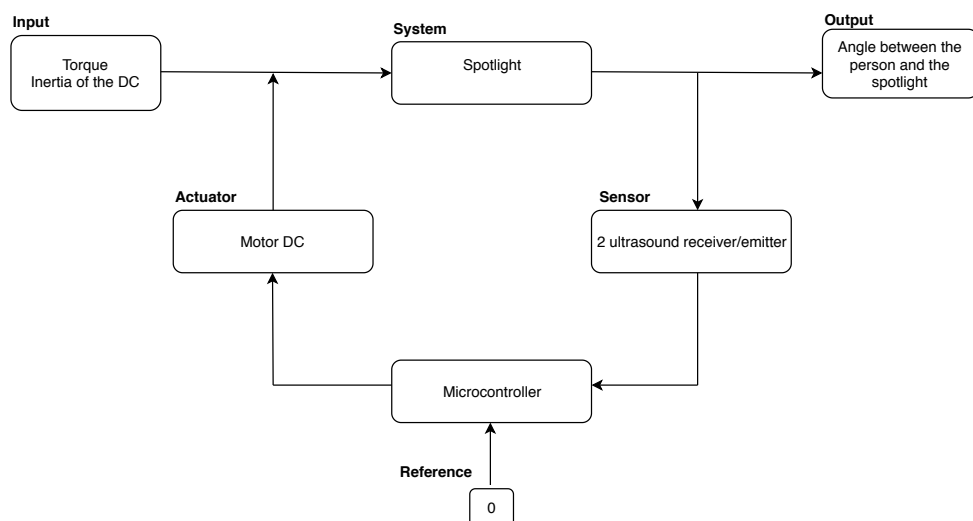


Figure 26: Block diagram showing the components of the whole system.

5.2 Open Loop System

The goal of this section is to describe the open loop system and thus to find its representation. This section aims also to make sure that the system is controllable and observable.

5.2.1 Schematic of the problem

- $\theta_r(d_1, d_2)$ is the reference angle. It depends on the distances d_1 and d_2 provided by the ultrasound sensors (position of the human body) placed on the motor shaft ;
- $\theta(t)$ is the instantaneous rotational angle of the spotlight (piloted by a DC motor). $\dot{\theta}$ is the angular speed of the motor and $\ddot{\theta}$ the angular acceleration ;
- p is the person moving in the room that the beam has to light ;

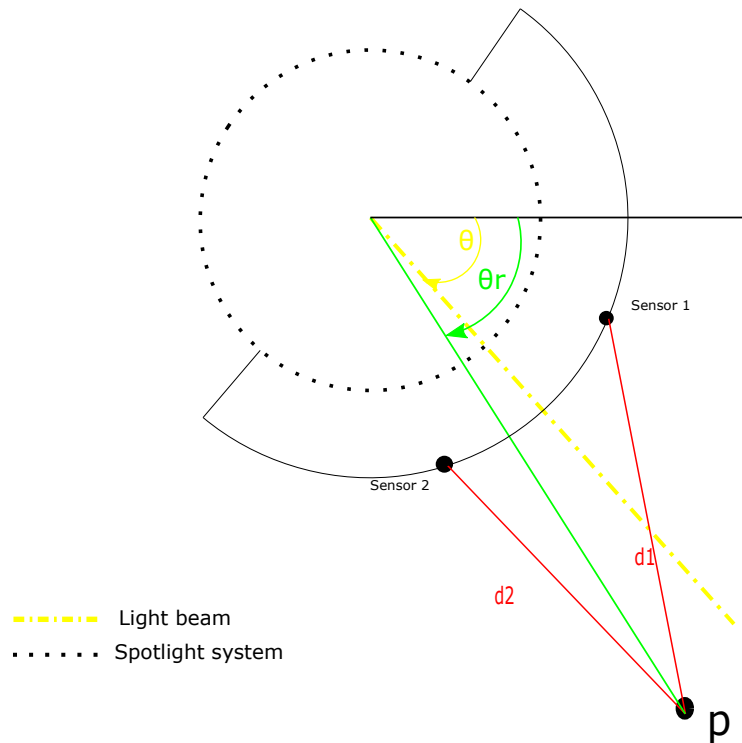


Figure 27: Schematic of the system for the system representation.

- T is the torque that the motor needs in order to rotate and follow the person. The following relationship can be used :

$$T = I\ddot{\theta}, \quad (1)$$

where I is the moment of inertia.

5.2.2 State-space representation

- State-variables : $\underline{x} = \begin{bmatrix} \theta \\ \dot{\theta} \end{bmatrix}$
- Inputs : $\underline{u} = \begin{bmatrix} \theta_r(d_1, d_2) \\ T \end{bmatrix}$
- Output : $y = \theta_r(d_1, d_2) - \theta(t)$

Using relationship (1) the matrices A , B , C and D can be found and used to represent the whole system :

- Update equation :

$$\dot{\underline{x}} = \begin{bmatrix} \dot{\theta} \\ \ddot{\theta} \end{bmatrix} = \begin{bmatrix} 0 & 1 \\ 0 & 0 \end{bmatrix} \underline{x} + \begin{bmatrix} 0 & 0 \\ 0 & \frac{1}{I} \end{bmatrix} \underline{u}$$

- Output equation :

$$y = [-1 \ 0] \underline{x} + [1 \ 0] \underline{u}$$

with $A = \begin{bmatrix} 0 & 1 \\ 0 & 0 \end{bmatrix}$, $B = \begin{bmatrix} 0 & 0 \\ 0 & \frac{1}{I} \end{bmatrix}$, $C = [-1 \ 0]$ and $D = [1 \ 0]$.

5.2.3 Simulations of the open loop system

The stability of the open loop system can be checked by computing the eigenvalues λ of the dynamic matrix A :

$$\det(A - \lambda I) = \begin{vmatrix} -\lambda & 1 \\ 0 & -\lambda \end{vmatrix} = 0$$

Solving the system gives $\lambda = 0$, so the system is unstable.

5.2.4 Controllability

The controllability matrix can be expressed as follows :

$$W_r = [B \ AB] = \begin{bmatrix} 0 & 0 & 0 & 0 \\ 0 & \frac{1}{I} & 0 & \frac{1}{I} \end{bmatrix}$$

The system is controllable because all the rows are linearly independent. Furthermore, an actuator is needed, i.e., the DC motor, because B has only one non-zero component.

5.2.5 Observability

In the same way as the controllability matrix, the observability one can also be computed. This last one is obtained as follows :

$$W_o = \begin{bmatrix} C \\ CA \end{bmatrix} = \begin{bmatrix} -1 & 0 \\ 0 & -1 \end{bmatrix}$$

The system is observable because all rows are linearly independent. The angle of the projector $\theta(t)$ is known at each time thanks to an angular sensor.

5.3 Frequency domain

5.3.1 Transfer function

The general formula in order to find the system transfer function is defined as :

$$H(s) = C(sI - A)^{-1}B + D$$

Using the matrices found in the open loop system the following transfer functions are obtained :

$$H_1(s) = 1 \text{ and } H_2(s) = \frac{-1/I}{s^2}$$

Because $u_2 = T$ is the controllable input only $H_2(s) = P(s) = \frac{-1/I}{s^2}$ is considered. The Bode diagram of $P(s)$ is represented in FIGURE 28.

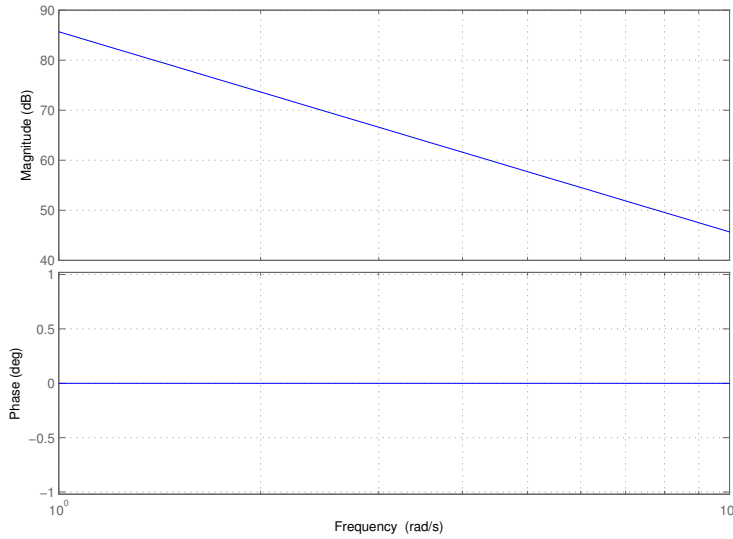


Figure 28: Bode Diagram of the system transfer function $P(s)$.

5.3.2 Constraints and design considerations

- **Ultrasound sensor delay**: the ultrasound sensor frequency is $f_{sensor} = 20\text{Hz}$, so it computes a distance each 50 ms ;
- **Angular sensor delay** : it computes an angle each 0.6 ms. This can be neglected compared to the ultrasound sensor delay ;
- **DC motor and microcontroller delays** are negligible ;
- **Maximum angle derivation** at which the light can illuminate the moving person : $15^\circ = 0.27 \text{ rad}$;
- **Maximum velocity** at which the motor can rotate : 30 RPM ;
- **Maximum DC motor torque** : $T_{max} = 2.45 \text{ Nm}$;
- **Constant moving person velocity** : approximately $5\text{km/h} \simeq 1.4 \text{ m/s}$;
- Let us assume that the spotlight system is a cylinder of height 10 cm, radius 10 cm and mass of 1kg. The weight of two ultrasound sensors are 10g and are located at 10 cm from the shaft :

$$I = \frac{1}{2} * 1\text{kg} * 0.01^2\text{m}^2 + 2 * 0.01\text{kg} * 0.01^2\text{m}^2 = 52.10^{-6}\text{kg.m}^2$$

- **System robustness** : System well designed such as it is robust to all the delays (high phase margin P_M) and reject noise as far as possible ;
- **Load disturbance**: having the angle of the spotlight θ as close as possible to the reference angle θ_r : if $|y| \leq 0.02 \text{ rad}$, the system tracks well the reference.

At which frequency does the system work ?

The system will work at a frequency f_{work} at which its frequency response must be as high as possible. In this case, it can be considered that the motor can follow maximum one oscillation of the moving person during one second: $f_{work} = 1\text{Hz}$. Thus it gives $\omega_{work} = 2\pi \text{ rad/s}$.

What could be a reasonable choice for the crossover frequency ?

The crossover frequency f_{co} corresponds to the frequency from which the system will never work, and thus attenuate its response. At this frequency the system responses has thus to be equal to 0dB. Since the frequency response has to be increased at the work frequency, i.e. at low ones, the crossover frequency has to be greater than f_{work} . Thus, we decided to take $f_{co} = 2f_{work} = 2\text{Hz}$, i.e $\omega_{co} = 8\pi \text{ rad/s}$, for example.

This choice will impact the system response but the system must remain feasible, i.e. the system constraints have to be respected : the torque must be less than the maximum torque, the tracking has to be good, the delays must be respected (if ω_{co} is too large, this condition can be unfulfilled), etc. All these constraints will thus be checked in the time domain, by observing what happens for the output y and the torque T when the closed-loop system is constructed. Also the results will be checked in the frequency domain by interpreting the bode diagram and the Nyquist plot.

Disturbance

The system has to be as reactive as possible to the movement of the moving person to light in the room. So, the simulations will be done by considering a disturbance that will correspond to different values that θ_r can take. A particular case where the person moves from the left to the right side of the room at a constant velocity (as specified in the constraints list) will be considered. From simulations the system reaction will be analyzed. FIGURE 29 shows the disturbance graph described just before.

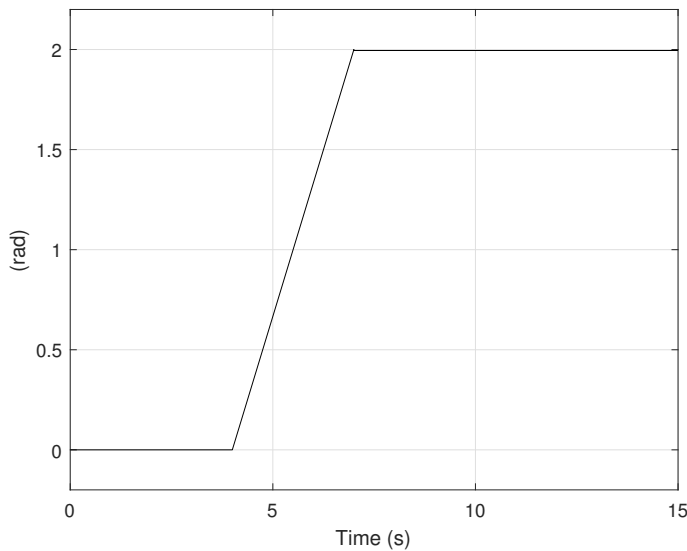


Figure 29: Disturbance shape used for the simulations.

5.3.3 Loop shaping

The system block diagram is represented in FIGURE 30. This last one is composed of several blocks that represent several things :

- r is the system reference ;
- The controller that will be added to our open loop system ;
- The actuator : the DC motor, described by its torque T ;
- The disturbance d defined previously, which represents the angle of the moving person in the room ;
- The system, described by its transfer function $P(s)$ also defined previously ;
- The sensors that will compute the distances d_1 and d_2
- The noise at a certain amplitude and a certain frequency, both unknown at first glance ;
- The system output $y = \theta_r - \theta$

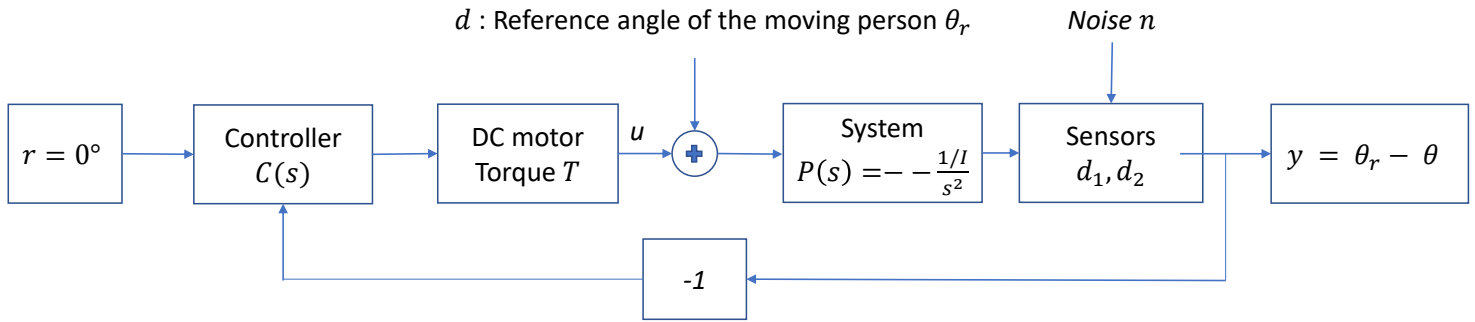


Figure 30: Block diagram of the closed-loop system.

Why implementing a controller?

The goal of the closed-loop system is to add a controller such as the system responds well. Indeed the system is expected to respond in a specific way : its frequency response has to be high at low frequencies, low at high frequencies, the gain has to be equal to 0 at the crossover frequency, any static error has to be removed, etc.

In order to see more concretely why a controller has to be added, the system step response can be represented, which is done in FIGURE 31. In this last one it can be seen that the system is obviously unstable, so it has to be compensated by added components. These will together correspond to the controller of the closed-loop system.

Closed-loop system transfer function

The robustness and the stability of the closed-loop system, which is represented in FIGURE 30, will be studied with a Nyquist approach. In this last one the properties of the loop transfer function $L(s) = P(s)C(s)$ will be studied, where $P(s)$ is the system transfer function and $C(s)$ the controller that will be designed in the next subsections, depending on the system considerations.

Delays

First of all, the delays that can affect the system have to be taken into account and are defined in the section "Constraints and Design considerations". The system delay robustness will be related to the phase margin of the closed-loop system transfer function. The higher the

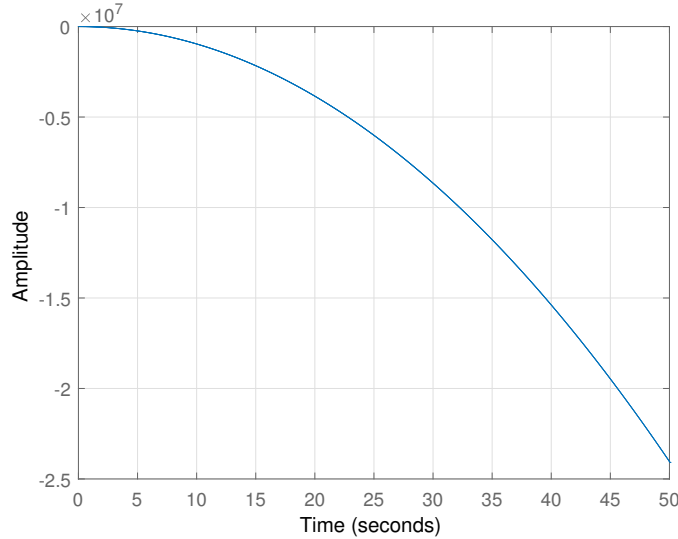


Figure 31: Step response in the open loop system.

phase margin the more robust our system is for the microcontroller, the sensors and the motor delays.

In order to represent the system total delay, a delay component will be added where the delay t_d will be equal to the sum of all the delays in our loop, i.e. 50ms as defined previously. The general form of this component can be written as follows :

$$G_{delay}(s) = e^{-t_d s} = e^{-0.05s}$$

The next step is to design the other components of the controller and then the Nyquist diagram will be represented in order to check that the system is stable, i.e. if the delays are well allowed in the loop shaping.

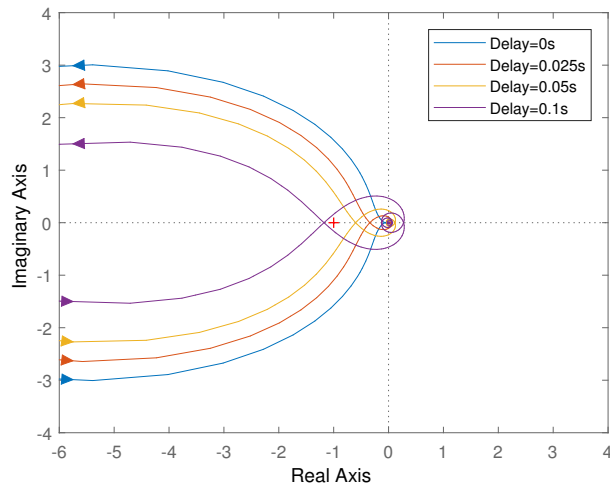


Figure 32: Nyquist plot for different delays.

Lead compensator

The lead compensator is used to increase the phase margin and flatten the system frequency response around ω_{co} . The general form of a lead compensator transfer function is such as :

$$G_{lead}(s) = G_{lead,0} \frac{1 + \frac{s}{\omega_z}}{1 + \frac{s}{\omega_p}},$$

where $\omega_z < \omega_p$. Three parameters have thus to be determined : $G_{lead,0}$, ω_z and ω_p where $\omega_z < \omega_{co} < \omega_p$ in order to have a phase margin P_M that is really high, and thus a system that is robust to delays caused by all the system components. Concerning the gain $G_{lead,0}$, this one has to be chosen such as the gain of the closed-loop transfer function $L(s)$ is equal to 0 at the crossover frequency ω_{co} .

In order to find the values of the 3 parameters, a trial-and-error procedure will be done with different values of phase margin P_M and the effects of choosing a higher or a lower P_M will be detailed.

So first of all let us sketch the bode diagram of the closed-loop transfer function of our system in which the lead compensator is added, with phase margins equal to 60, 70 and 80 degrees. This plot is represented in FIGURE 33.

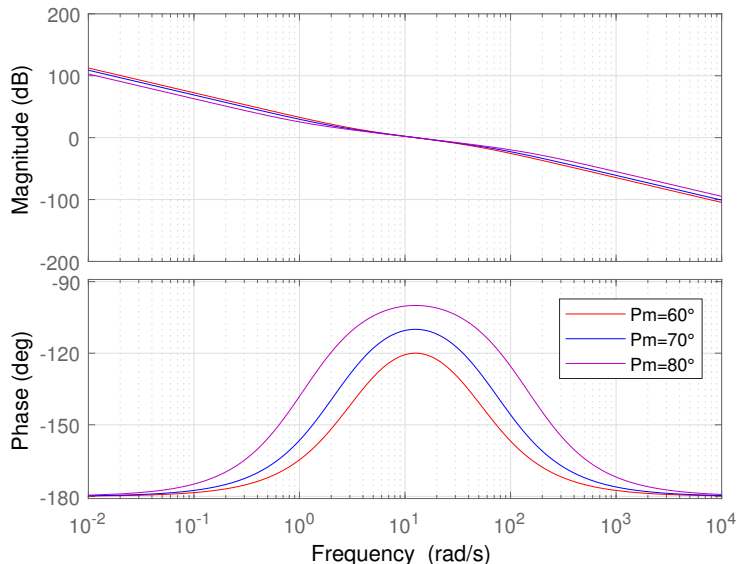


Figure 33: Bode diagram of $L(s)$ with the added lead.

In this last one it can be seen that the the more ω_z and ω_p are far from each other the more the phase margin. In fact the pole ω_p will cause a phase decrease of 90 degrees and the zero ω_z a phase increase of 90 degrees. So taking them farther from each other the phase in the frequency range $[\omega_z; \omega_p]$ will increase and thus the phase margin will increase as well.

The other effect is that the farther ω_z and ω_p are from each other the higher the magnitude bode diagram at high frequencies and low at high frequencies. But in practice the frequency response at high frequencies has to be low and the high at low frequencies. So since the phase margin has to be high a lag compensator would maybe be added in addition to the lead one in order to increase the gain at low frequencies and thus compensate this effect caused by the lead. Concerning the effect at high frequencies a low-pass filter can be used in order to compensate the effect of the lead at high frequencies.

Concerning the results in the time domain the 3 cases for the different phase margins are represented in FIGURE 34 and 35. These ones represent respectively the reference tracking of the chosen disturbance and the motor torque,i.e. the controllable input.

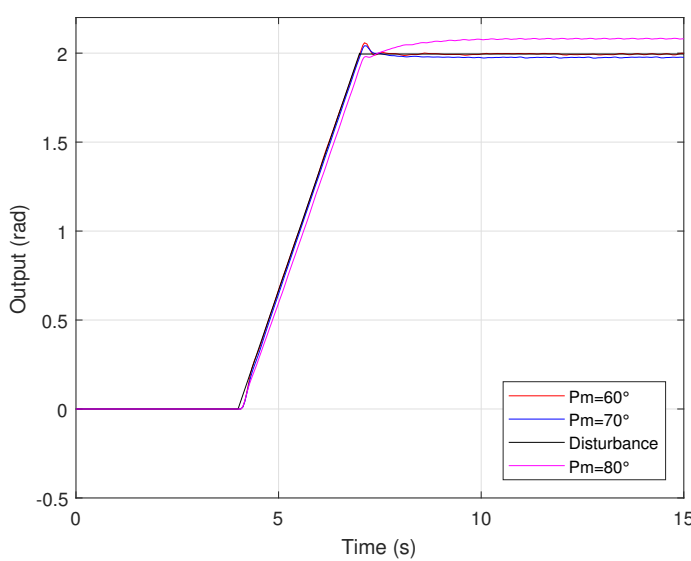


Figure 34: Reference tracking with the added lead.

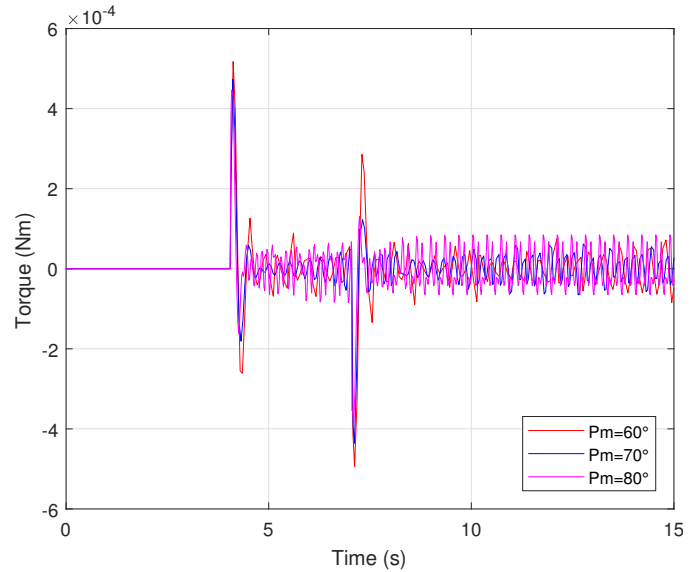


Figure 35: Motor torque with the added lead.

In the first one it can be noticed that the 3 cases cause a peak when the amplitude reaches 2 radians and then the signal reaches a constant value. This is thus caused by the slope change of the disturbance. Indeed the motor has nothing more to track so this change in slope will always cause a peak. Let us note that the lower the phase margin the higher the peak. This effect has thus to be taken into account for the phase margin final choice.

The second observation is that the more the phase margin the more important the static and tracking errors. Indeed in the worst case where the phase margin is equal to 80 degrees the tracking error can be seen when the slope is positive, i.e. during the tracking of the moving person that walks from 0 to 2 radians in the room. A static error appears also when the person stays at the position 2 radians and stops its motion. This effect is not problematic since an added lag compensator can have as advantage to get rid of any static or tracking error.

Concerning the motor, the only thing to care about is to check if its torque is not too high and thus to check if its maximum value respects the constraint. Indeed it has to be lower than the value $T_{max} = 2.45$ and in this case the maximum torque is about 5^{-4} Nm in absolute value. This value is well lower than T_{max} and therefore there is no problem concerning the motor torque, whatever the phase margin. Let us note that for a 70 degrees phase margin, the oscillations are less important than for other cases.

Results, effects and conclusion

As a summary, if the phase margin P_M increases some effects are visible in the bode diagrams and in the time domain graphs represented previously.

On the one hand, if PM is increased the gain is increased at high frequencies and attenuated at low ones, which is not what is wanted to do in the design. Moreover the higher the phase margin the higher the static and tracking errors and the higher the peak when the slope changed. But on the other hand, the more the phase margin the more delays can be accepted in the closed-loop system.

In conclusion, we have thus decided to add a lag compensator in the controller in order to remove the static and tracking error and reduce the peak. Without the lag, the graph with a

60 degrees phase margin can be acceptable, but there are oscillations and the first peak is too high in the reference tracking. Thus we will try to obtain better results with the added lag.

Lag compensator - PI controller

In general a lag compensator is useful when the gain at low frequencies has to be increased, in order to make the system more reactive, so it decreases the phase margin. However adding such a component can bring some instabilities. Thus, depending on the chosen parameters, a trade-off can be made between making the system more reactive and reducing the peak that appears when the slope of the disturbance changes.

The general equation is similar to the one developed for the lead compensator :

$$G_{lag}(s) = G_{lag,0} \frac{1 + \frac{s}{\omega_z}}{1 + \frac{s}{\omega_p}},$$

except that here $\omega_z > \omega_p$.

The position of the lag pole depends thus on the values of ω_p . In this case the system has to get rid of its static and tracking errors and thus its reference tracking has to be improved. This can be done by increasing the gain at low frequencies, since the system works at these ones. To do so a PI controller is used. The only difference between this controller and the lag controller is that the PI one has its pole at the frequency 0Hz. The other motivation to put a PI controller rather than a lag compensator is linked to the phase bode diagram. Indeed if the pole is at 0rad/s, the phase will thus begin to -90 degrees, and then increase till 0 degree around ω_z . Adding a lag compensator can decrease the phase margin, but with a PI controller where ω_z is much smaller than ω_{co} , the phase margin will not really be affected, which is wanted.

In general the PI controller transfer function can be written as follows :

$$G_{PI}(s) = k_p + \frac{\omega_z}{s} = \frac{s + \omega_z}{s},$$

where k_p has been taken equal to 1 in order to keep the frequency response in magnitude equal to 0 at the crossover frequency ω_{co} .

The only parameter to choose is thus ω_z . In the "Signals and systems modeling" course it was explained that when there is a zero equal to ω_z , the phase will be equal to 0 degree when the frequency is higher than $10 \times \omega_z$. The choice $\omega_z = 10 \times \omega_{co}$ has thus been made in order to apply what was explained before and thus obtain ω_z much smaller than ω_{co} . By this way the phase margin will not be really affected by the PI controller.

The resulting bode diagram of the closed-loop transfer function is represented in FIGURE 36. In this last one the values of the pole and the zero of the lead have been adapted in order to always obtain the peak of the phase plot at the crossover frequency. It can also be noticed that the gain at low frequencies has been amplified compared to the bode diagram without the lead compensator.

The reference tracking and the motor torque plots with the added PI controller have been both represented in FIGURES 37 and 38 respectively.

In the first one some effect can be observed. The first one is that for low phase margins the tracking and static errors have been removed. However oscillations appear in the case where the phase margin is equal to 60 degrees, which is a bad consequence caused by the added PI controller. For the phase margin equal to 80 degrees, the tracking error is still present and

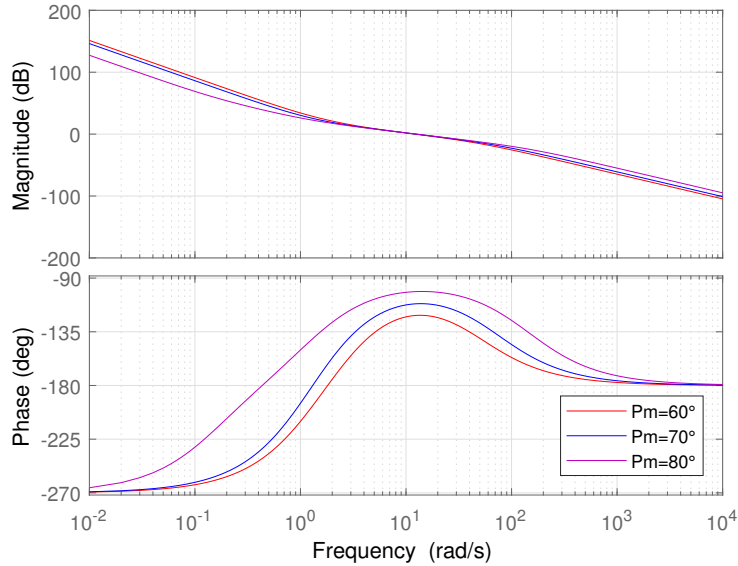


Figure 36: Bode diagram of $L(s)$ with the added PI controller.

the static error seems to decrease when the time tends to infinity. The system is not reactive enough and this phase margin can not been chosen in our case.

Concerning the motor torque there is nothing more to describe about it compared to the comments made in the lead compensator section. This one is always smaller than the maximum allowed torque that the motor can apply and thus this constraint is well respected. It can be observed that as without the PI controller when the phase margin is equal to 70 degrees there is less oscillations.

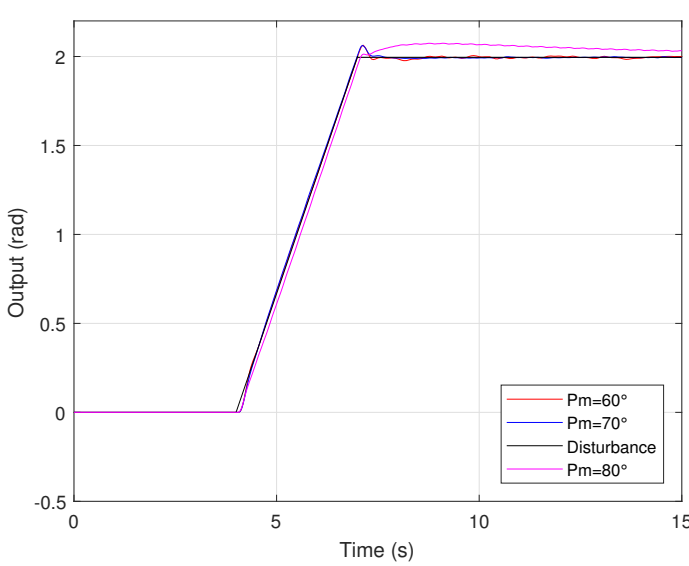


Figure 37: Reference tracking with the added PI controller.

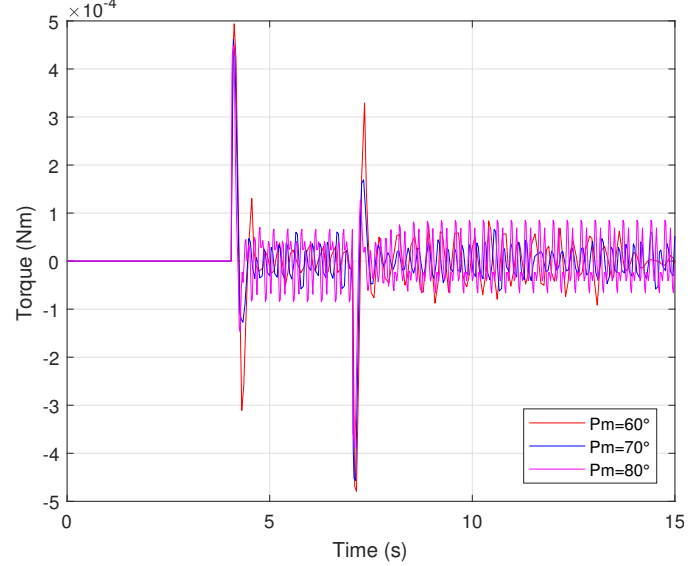


Figure 38: Motor torque with the added PI controller.

Results, effects and conclusion

As summary, if P_M decreases, different effects appear in the bode diagram of the closed-loop system transfer function $L(s)$ and the time domain graphs.

On the one hand, the system more reactive and converges thus faster to the disturbance. Also the less the P_M the more the static and tracking errors are attenuated. Also it has been observed that in this case the gain is attenuated at high frequencies and amplified at low ones.

On the other hand the only drawback is that if P_M decreases too much, some oscillations can appear in the reference tracking and thus the motor will follow less good the moving person in the room.

A trade-off has thus to be made and the best choice was thus to keep the PI controller and choose a phase margin P_M equal to 70 degrees. Indeed FIGURE 39 represents a zoom in the tracking error and from this last one it can be observed that without the PI controller the tracking is less good than with this component. In fact even if the peak at the slope change has been increased a little bit the static error is not present anymore and the system is more reactive.

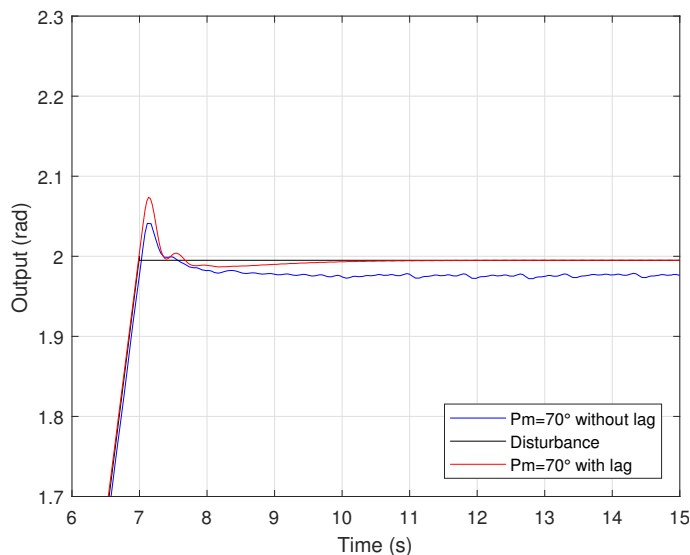


Figure 39: Comparison between the temporal graphs with and without lead.

Low-pass filter

The goal of adding a low-pass filter in the controller is to reject the noise at high frequencies, so the gain after the crossover frequency is reduced. The general transfer function associated to a low-pass filter can be written as follows :

$$G_{HF}(s) = G_{HF,0} \frac{1}{\frac{s}{\omega_{HF}} + 1},$$

where ω_{HF} is the cutoff frequency of the filter.

For example $\omega_{HF} = 10\omega_{co}$ can be chosen in order to affect only high frequencies, i.e. the ones that are greater than the crossover frequency. In order to be sure that this choice is the best two more cases are represented : one where the cutoff frequency of the low-pass filter is less than $10\omega_{co}$ and another one where the cutoff frequency is a little bit higher than this value. Concerning the gain $G_{HF,0}$ this last one will be equal to 1 in order to keep the gain of $L(s)$ equal to 0 dB at the crossover frequency, which has been taken into account in the design of the lead compensator block.

Let us note that normally the closed-loop system has already a low gain at low frequency because its transfer function is inversely proportional to s^2 , so a low-pass filter is not really necessary. But the added lag in the controller has increased the gain at these frequencies so a low-pass filter will be implemented.

The resulting bode diagram of the closed-loop transfer function is represented in FIGURE 40. In this last one it can be noticed that the higher the low-pass cutoff frequency the more the phase margin. Let us note that the values of the pole and the zero of the lead compensator have been adapted again in order to obtain the peak of the phase bode diagram at the crossover frequency. By this way the maximum phase margin is obtained with the corresponding cutoff frequencies.

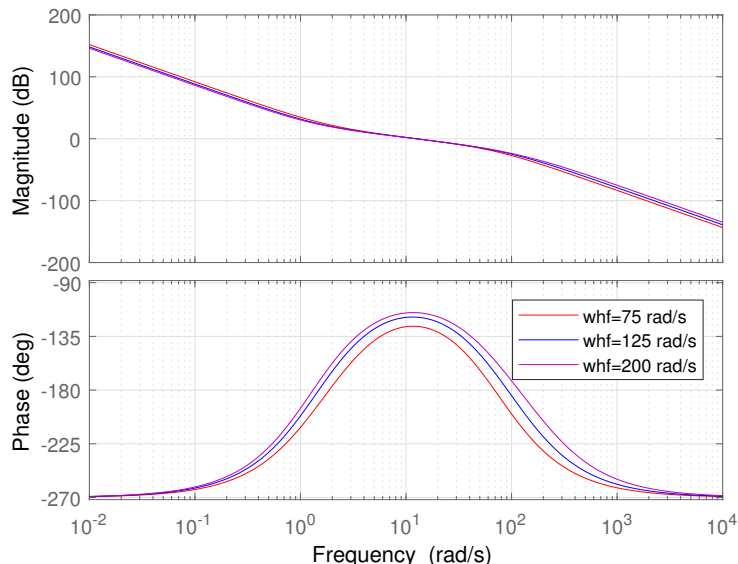


Figure 40: Bode diagram of $L(s)$ with the added LP filter.

Concerning the time domain graphs both are represented in FIGURES 41 and 42. The first one represents the reference tracking. The only effect of changing the cutoff frequency can be observed in the case when this last one is equal to 75 rad/s. In this case it can be observed that oscillations begin to appear and thus the tracking is not good anymore. Thus the cut-off frequency that will be chosen has not to be too small.

The second figure represents the evolution of the motor torque as a function of time. From this graph it can be observed that if the cutoff frequency is too small or too large, oscillations' magnitude increases. Despite that, the constraint concerning the maximum motor torque is respected for all cut-off frequencies that were chosen.

Results, effects and conclusion

As summary, the choice of the low-pass filter cutoff frequency will be done based on a trade-off, as for the other components.

Indeed if ω_{HF} decreases, high frequencies are more attenuated but the drawbacks are that the phase margin P_M will decreased and oscillations can appear in the reference tracking if the cutoff frequency is too small. Also for the cases where ω_{HF} was too high or too slow bigger oscillations appeared in the motor torque graph.

Finally we have thus decided to choose the initial value of the cutoff frequency, i.e. $\omega_{HF} = 125\text{rad/s}$.

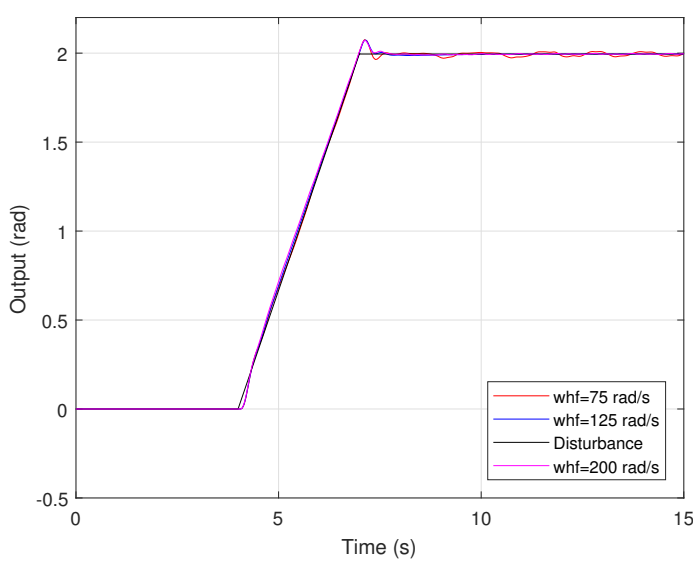


Figure 41: Reference tracking plot with the added LP filter.

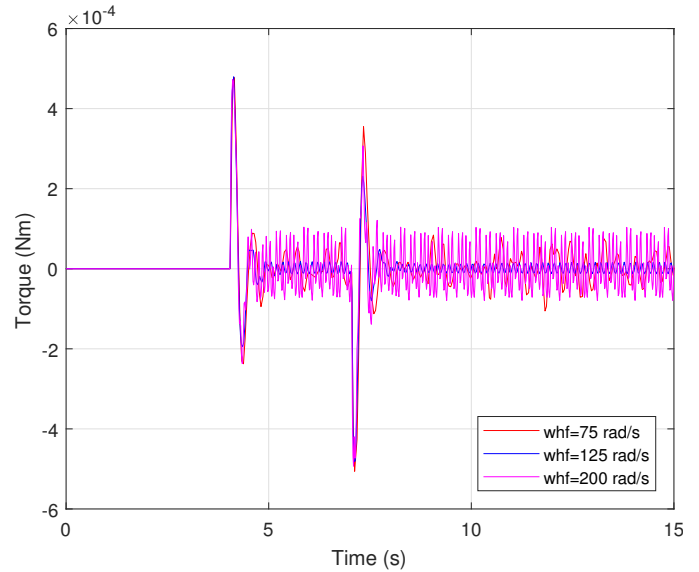


Figure 42: Motor torque with the added LP filter.

5.3.4 Final controller

The final closed-loop system transfer function is thus given by all the previous blocks put in series. The multiplication of all their transfer functions gives the final controller transfer function. The resulting closed-loop system transfer function can be expressed as follows :

$$L(s) = C(s)P(s)$$

where

$$C(s) = G_{delay}(s)G_{lead}(s)G_{lag}(s)G_{HF}(s)$$

The resulting bode diagram, Nyquist plot, reference tracking and motor torque plots are all represented in FIGURES 43, 44, 45 and 46 respectively.

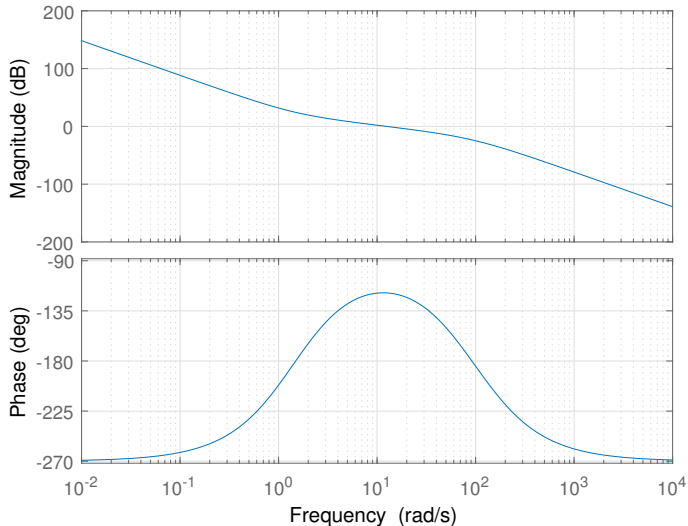


Figure 43: Bode diagram of $L(s)$.

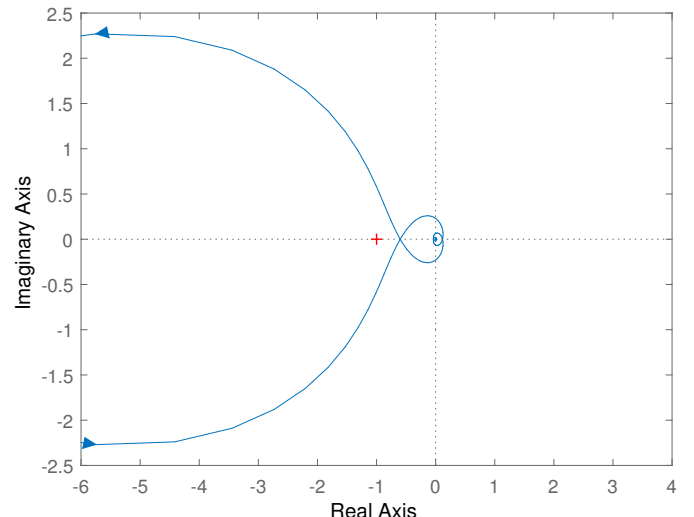


Figure 44: Nyquist plot of $L(s)$.

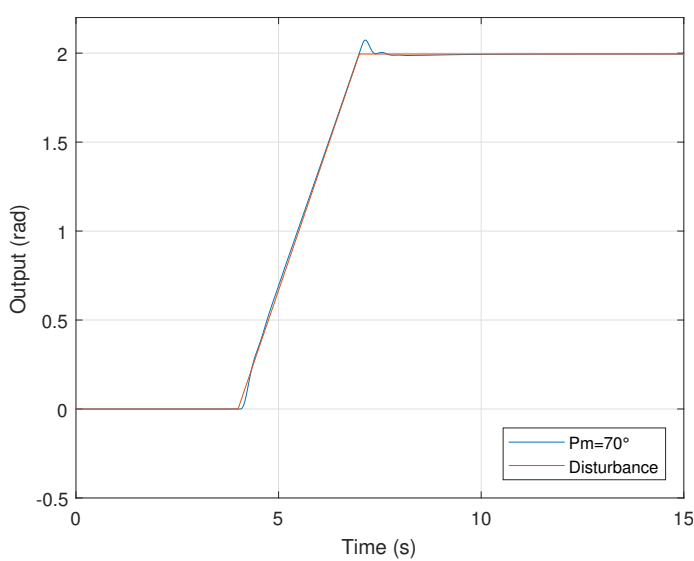


Figure 45: Reference tracking in the closed-loop system.

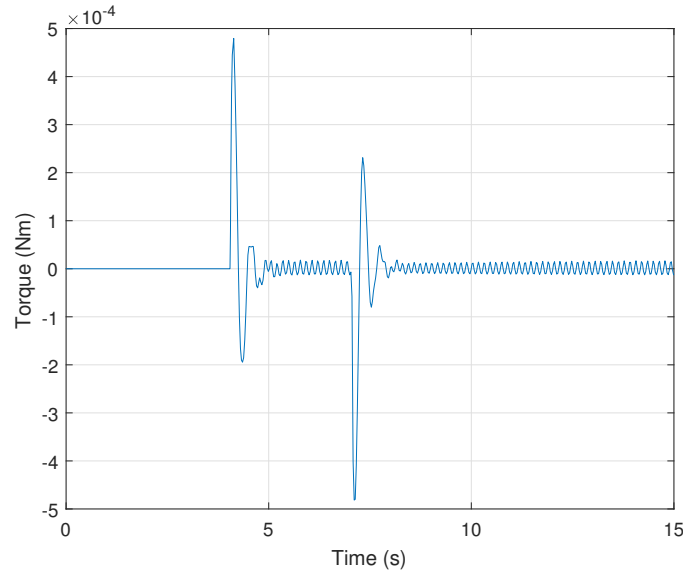


Figure 46: Motor torque evolution in the closed-loop system.

Constraints and Design considerations : check

Now with the resulting plots the constraints listed previously are described again and are checked :

- Total system delay $\simeq 50\text{ms}$: The Nyquist plot is stable since the closed contour $L(s)$ for all the values ω has no net encirclement of $s = j\omega = -1$.
- Maximum DC motor torque $T_{max} = 2.45\text{Nm}$: Always respected.
- Track the reference $r = 0$ as well as possible ($y \leq 1\text{degree} = 0.02\text{rad}$) : Not valid for the peak when the slope of the disturbance changes, but otherwise it is the case so the system tracks well the reference ;
- The system reactive and has no static error.

Concerning the peak when the slope changes, the best one has been obtained. Indeed at this moment the person is not moving anymore so the motor has to stop moving also. Thus the peak can not be reduce in order to respect the constraint over the reference tracking. But since the peak is not too high and appears during less than 1 second this one is accepted anyway.

As expected the closed-loop gain is high at low frequencies, thus around f_{work} too and it is attenuated at high frequencies, i.e. at frequencies higher than ω_{co} , in order to reject as much noise as possible. At low frequencies the system has to be reactive to the disturbance and it has to track the reference as well as possible. These conditions will be studied in the "Gang of "2"" analysis⁴. This last one can be found in the Appendix.

5.3.5 Noise

Finally, the effect of adding some noise can be analyzed. An alternative noise at the network frequency 50Hz can be consider. Indeed our system will be directly connected to the network,

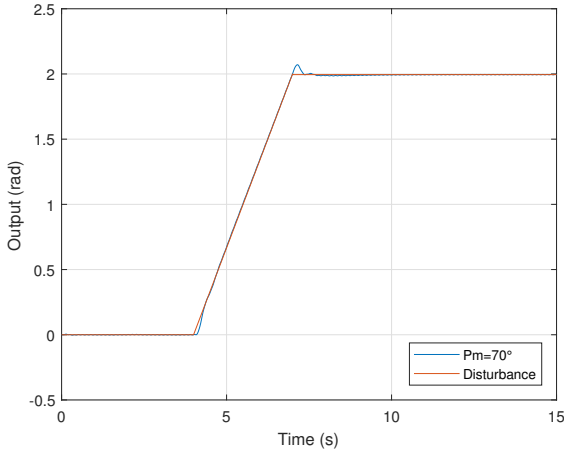


Figure 47: Reference tracking with the noise.

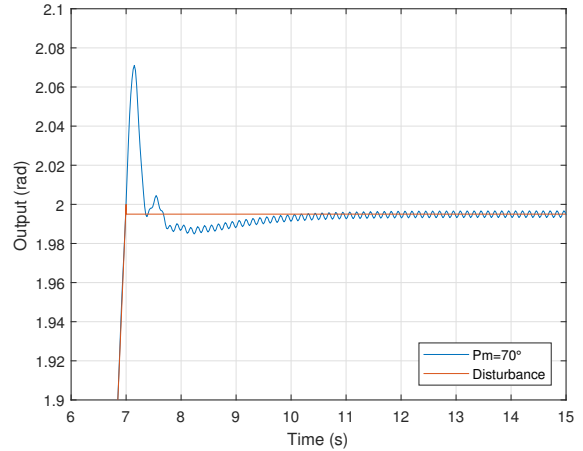


Figure 48: Zoom in the reference tracking with the noise/

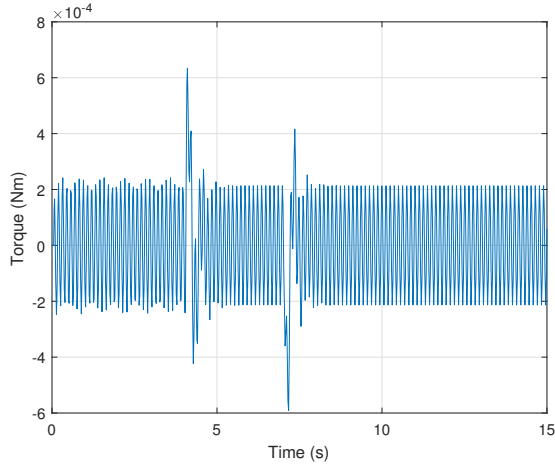


Figure 49: Motor torque with the noise.

so most parasites will be at a frequency corresponding to the network frequency.

It can be observed in the graphs represented in FIGURES 47, 48 and 49 that the presence of noise causes only more oscillations in the time domain. Even if more oscillations appear the system constraints are still respected. We can conclude that the system is well design and is robust against the noise.

⁴Only two functions of the gang of four have been analyzed, since the two others depend on $S(s)$ that is analyzed here.

5.4 Implementation of the controller

5.4.1 PID controller

Our final controller has the following form :

$$\begin{aligned} C(s) &= G_{delay}(s)G_{lead}(s)G_{PI}(s)G_{HF}(s) \\ &= e^{-t_{ds}}G_{lead,0}\frac{1 + \frac{s}{\omega_z}}{1 + \frac{s}{\omega_p}}\frac{s + \omega_z}{s}G_{HF,0}\frac{1}{\frac{s}{\omega_{HF}} + 1} \\ &= e^{-0.05s}0.0011\frac{1 + \frac{s}{1.666}}{1 + \frac{s}{71.82}}\frac{s + 1.25}{s}\frac{1}{\frac{s}{125} + 1} \end{aligned}$$

Since the delays are intrinsic of our system the controller to implement is the following one

:

$$\begin{aligned} C(s) &= G_{lead}(s)G_{PI}(s)G_{HF}(s) \\ &= 0.0011\frac{1 + \frac{s}{1.666}}{1 + \frac{s}{71.82}}\frac{s + 1.25}{s}\frac{1}{\frac{s}{125} + 1} \end{aligned}$$

It is asked to design a PID controller and thus $C(s)$ will be expressed as follows :

$$G'_{PID}(s) = G'_{PI,\infty}(s)\left(1 + \frac{\omega_{PI}}{s}\right)G'_{PD,0}(s)\frac{1 + \frac{s}{\omega_{PD}}}{1 + \frac{s}{\omega_p}},$$

This is the multiplicative form of a PID controller. In this expression there are one PI controller and one PD controller. The PD controller corresponds to the lead compensator. Thus we have decided to not consider the low-pass filter. FIGURE 50 shows the controller $C(s)$ and this last one without the low-pass filter.

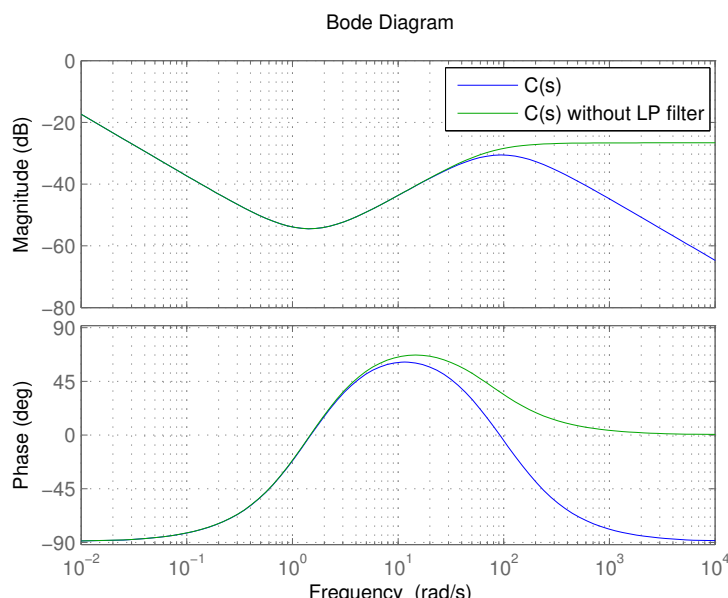


Figure 50: Controller $C(s)$ with and without the low-pass filter.

The controller expression becomes :

$$\begin{aligned} C(s) &= G_{lead}(s)G_{PI}(s) \\ &= 0.0011 \frac{1 + \frac{s}{1.666}}{1 + \frac{s}{71.82}} \left(1 + \frac{1.25}{s}\right) \end{aligned}$$

And thus

$$\begin{aligned} C(s) &= G'_{PID}(s) \\ \Leftrightarrow 0.0011 \frac{1 + \frac{s}{1.666}}{1 + \frac{s}{71.82}} \left(1 + \frac{1.25}{s}\right) &= G'_{PI,\infty}(s) \left(1 + \frac{\omega_{PI}}{s}\right) G'_{PD,0}(s) \frac{1 + \frac{s}{\omega_{PD}}}{1 + \frac{s}{\omega_p}} \end{aligned}$$

The values for the parameters of the PID controller can thus be computed :

$$\begin{aligned} G'_{PI,\infty}(s)G'_{PD,0}(s) &= 0.0011 \\ \omega_{PD} &= 1.666 \\ \omega_p &= 71.82 \\ \omega_{PI} &= 1.25 \end{aligned}$$

In the microcontroller the following equation will be implemented :

$$u[k] = K_p e[k] + u_i[k - 1] + K_i e[k] + K_d(e[k] - e[k - 1]),$$

where $e[k]$ is the error.

The z-transform of the previous equation gives the transfer function of the PID controller :

$$G_{PID}(z) = \frac{U(z)}{E(z)} = K_p + K_i \frac{1}{1 - z^{-1}} + K_d(1 - z^{-1}),$$

where $U(z)$ and $E(z)$ are the z-transforms of $u[k]$ and $e[k]$ respectively.

Using the bilinear mapping, the previous equation can be rewritten as follows :

$$G'_{PID}(s) = \frac{U(s)}{E(s)} = K_p + \frac{K_i}{T} \frac{1 + \frac{s}{\omega_p}}{s} + K_d T \frac{s}{1 + \frac{s}{\omega_p}},$$

where $\omega_p \triangleq \frac{2}{T} = 71.82$ thus $T = \frac{2}{\omega_p} = 0.0278$ s. This equation corresponds to the additional form of the PID controller and from this form the multiplicative one can be found.

In order to find the coefficients K_p , K_d and K_i the following relationships can be used :

$$\begin{aligned} K_p &= G'_{PI,\infty}(s)G'_{PD,0}(s) \left(1 + \frac{\omega_{PI}}{\omega_{PD}} - 2 \frac{\omega_{PI}}{\omega_p}\right) = 0.0019 \\ K_i &= 2G'_{PI,\infty}(s)G'_{PD,0}(s) \frac{\omega_{PI}}{\omega_p} = 3.7658 \cdot 10^{-5} \\ K_d &= \frac{1}{2} G'_{PI,\infty}(s)G'_{PD,0}(s) \left(1 - \frac{\omega_{PI}}{\omega_p}\right) \left(\frac{\omega_p}{\omega_{PD}} - 1\right) = 0.0224 \end{aligned}$$

The resulting PID controller computed with the coefficient values just above is shown in FIGURE 51 with the controller $C(s)$ without the low-pass filter.

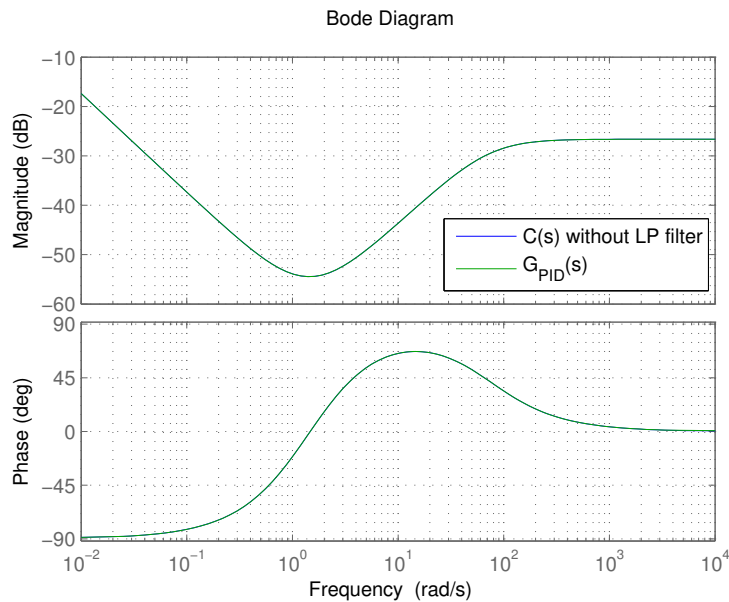


Figure 51: Controller $C(s)$ without the low-pass filter and the PID controller.

5.4.2 Implementation of the controller

Concerning the implementation of the controller, the description can be found in **section 3.5.3** (embedded part).

5.4.3 Conclusion

As a conclusion several main points have been discussed in this part.

First the system to study is described as well as its representation. The corresponding parameters such as the inputs, the output, the reference, the actuator and the sensors have been described as well.

The second section was dedicated to the study of the described system. Its A, B, C, D representation has been described and this has allowed to determine the characteristic of the system. We have concluded that the system was unstable, controllable and observable.

Then a frequency analysis has been done. In this last one a controller has been designed and thus the closed-loop system has been entirely described. This last one allows thus to well track the reference, in order to always have our output that tends to 0. Also the system has been designed such as the disturbance do not affect the input and the output and such as the noise was rejected at high frequencies.

Finally the controller has been implemented in practice and the resulting simulations have been illustrated and commented in the "embedded part" section.

6 Mechanics and hardware

FIGURE 52 shows a view on the device in its whole. It consists of a wooden structure that links all the components of the system together, mounted on a metal stand.



Figure 52: Projector in its whole.

6.1 Motor shaft, angular sensor and ultrasound sensor

One challenge was to fix the motor shaft with the shaft supporting the ultrasound sensors (as shown in FIGURE 52) and with the angular sensor. Fortunately, our motor has a shaft going through its 2 sides (as shown in FIGURE 54), so we could couple the angular sensor on one of the two and the ultrasound sensors on the other. The static part of the angular sensor is secured in place, fixed on one of the wooden plated.

For the angular sensor it was quite simple, the angular sensor was attached to the motor shaft by a shaft coupler, as shown in FIGURES 55 and 56.

For the shaft supporting the ultrasound sensors it was more complicated, the diameter of the motor shaft has a diameter too small to produce enough friction to move the whole mass of the wooden shaft. We tried to screw through the wood, but by turning, the wood was wearing down and there was less and less friction. So finally, we drilled in the wood of a diameter smaller than the diameter of the motor shaft, and we pushed it in and then we took the strong glue, which is an irreversible solution and enough but it turned out to be the best solution.

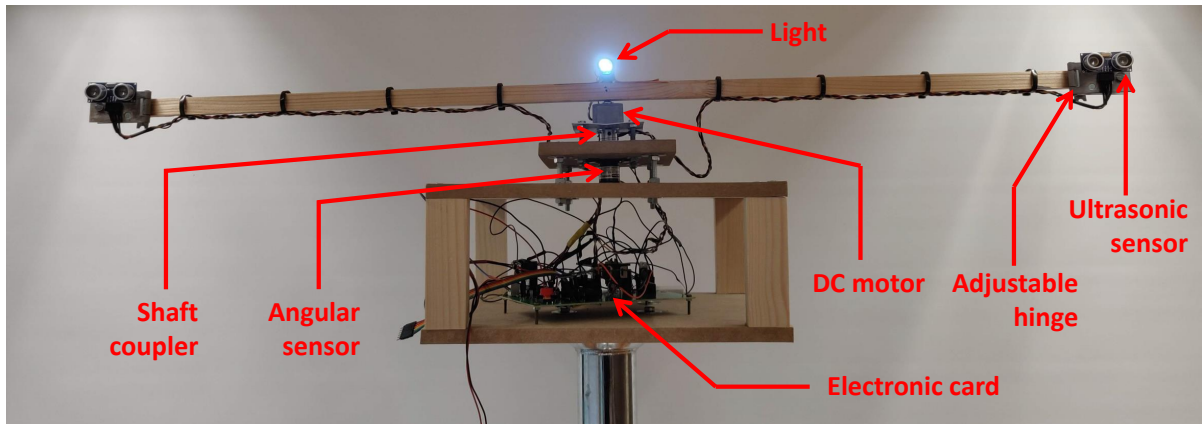


Figure 53: Zoom on the projector system.



Figure 54: Motor.



Figure 55: Angular sensor.



Figure 56: Motor shaft.



Figure 57: Ultrasound sensor.

6.2 PCB design

In order to avoid electrical problems due to bad soldering and to reduce the effect of electromagnetic noise, a PCB has been designed. This last one has been designed using EasyEDA, an online PCB editor with access to many user-designed schematics and footprints. FIGURE 58 shows a view of the PCB.

The PCB design has two layers. The top layer is displayed in FIGURE 59 and the bottom layer in FIGURE 60. Both of the layers have a copper ground plane. A single layer PCB would probably have been possible for this circuit. However, it would almost certainly require the use of external cables to implement some of the connections.

For the design of the circuit, we tried to separate the power part and the control part as much as possible. Getting the disruptive components such as the coil as far as possible from the control part allows to reduce potential errors due to noise at the microcontroller. Also, we do not want self-heating component such as the linear regulator LM or the H-bridge too close to the microcontroller.

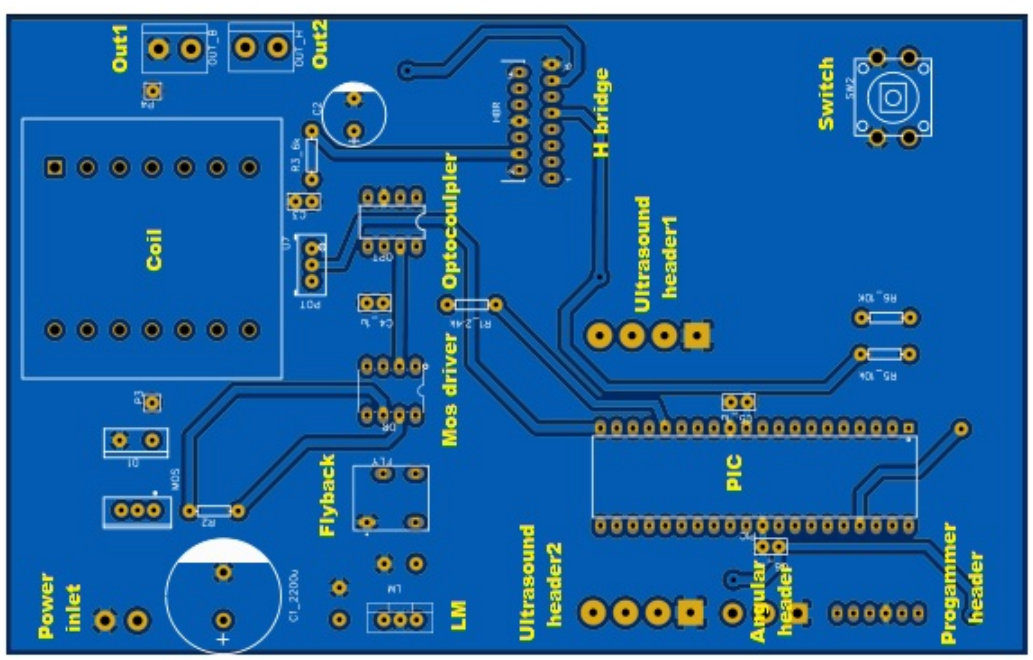


Figure 58: PCB design.

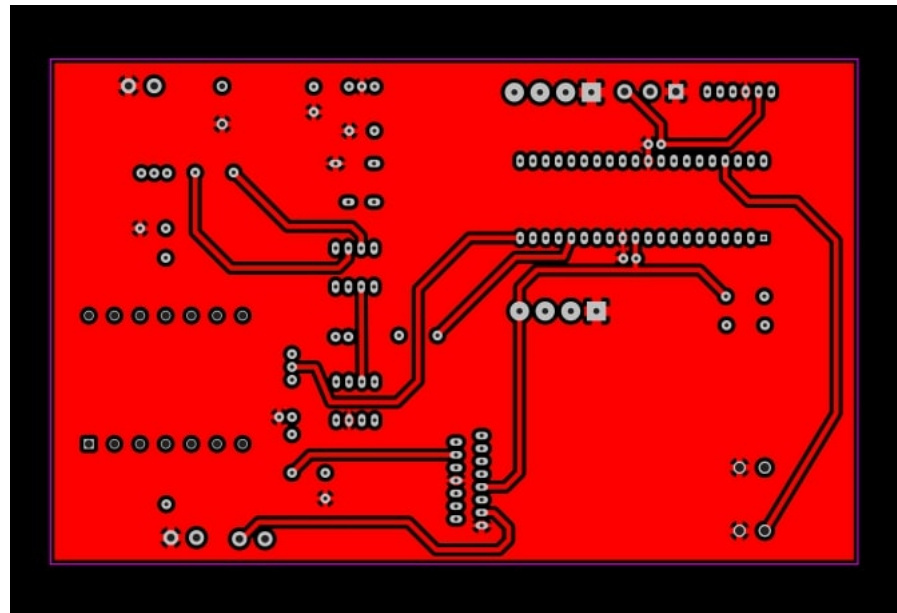


Figure 59: Top layer of the PCB.

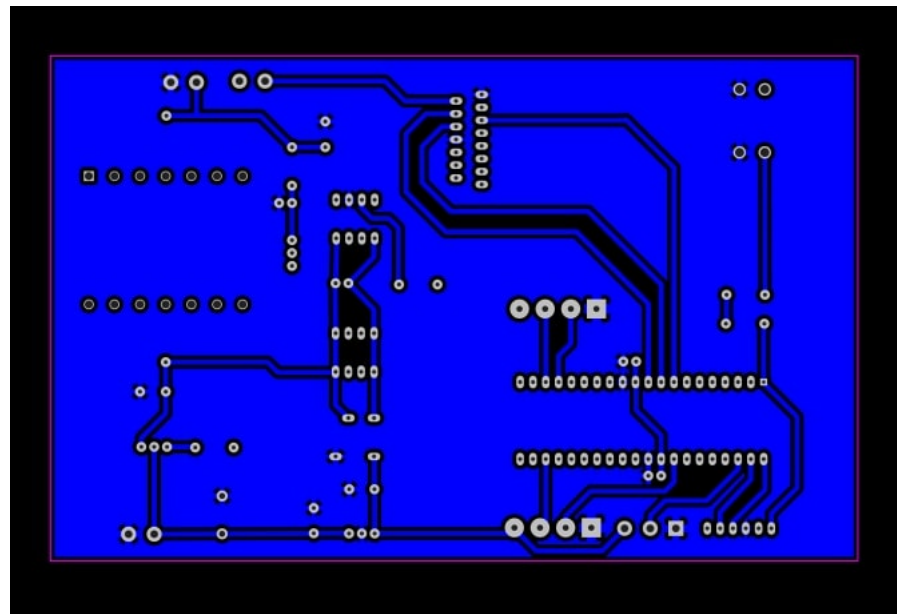


Figure 60: Bottom layer of the PCB.

6.3 Orientation of the ultrasonic sensors

The problem of the orientation of the sensors was solved by using hinges as supports for the sensors, which makes their aiming direction adjustable in order to select an optimal orientation. In order to maximize the surface where the sensors both work, i.e. the area where the motion tracking is functional, the sensors datasheet was used. From FIGURE 61, it can be seen that the cone of most effective measurements has an amplitude of 30° , whereas the total amplitude of the measuring angle is of about 60° (for lower distances on the edges). Based in this data, the

sensors orientation was adapted at 30° from their support. This way, as shown in FIGURE 62, it ensures a wide region of detection, that is 1 meter wide, which ensures to not lose the moving target when tracking. However, after testing, it appeared that a more appropriate value for the sensors orientation is of about 20° , since it gave better results. This is due to the fact that the sensors directionality is reduced in practice, because of real life constraints such as sound absorption in clothes.

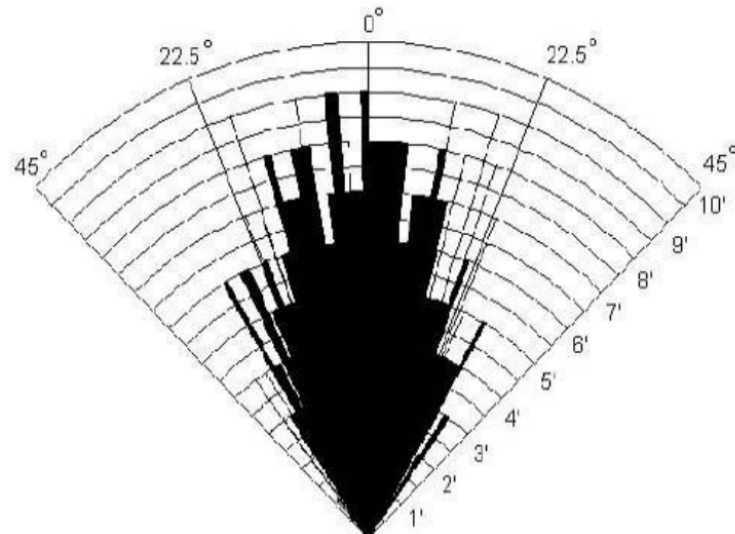


Figure 61: Directionality graph of the HC-SR04 ultrasonic distance sensor.

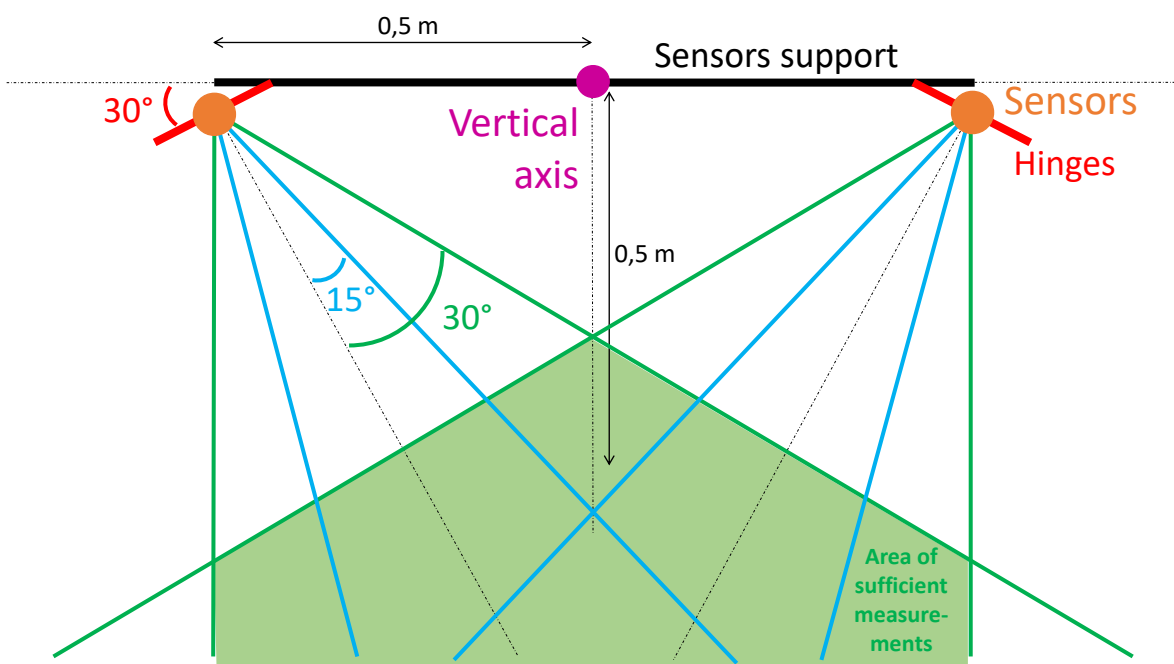


Figure 62: Illustration of the chosen orientation for the distance sensors.

7 Improvements

If we have enough time, some improvements can be done on our system. These are listed below :

- Adjusting the width of the light beam as a function of the distance between the person and the projector : the closer the person is to the projector, the wider the angle of the light beam ;
- Turning the light off when nobody is detected ;
- Flashing the light if the person is too close.

8 Conclusion

As a conclusion we managed to finally design our wanted project. First theoretically in the linear control systems part and then practically in the embedded system part. We also realize the implementation of a feedback loop in a supply made by ourselves in the power electronics part.

To conclude this major project we can say that this project gave us different skills :

The management part taught us to organize ourselves, to be efficient and to manage better the group work which is important for engineers. We also learned about bases in project management to be able to handle the completion of any project.

The linear control systems part taught us how to synthetize and simulate any system. This part is very useful in practice to not waste money in experiments and prefer to first go through a theoretical representation of the system and to be able to control.

The electronic power part allowed us to design a power supply from the beginning to the end, which allowed us to familiarize ourselves with a lot of concepts, and put into practice skills acquired theoretically during the first quadrimester.

Finally the embedded part was the part that connected all the parts together, from the implementation of a feedback loop for the feeding of our buck to the implementation of the projector system. It also allowed us to distinguish the theoretical simulations and the practical results. From this we learned that sometimes the theoretical representations are complicated to implement and we have to make simpler model in practice. We also learned about some others skill like a PCB design and mechanical stuffs.

9 Appendix

9.1 Project planning

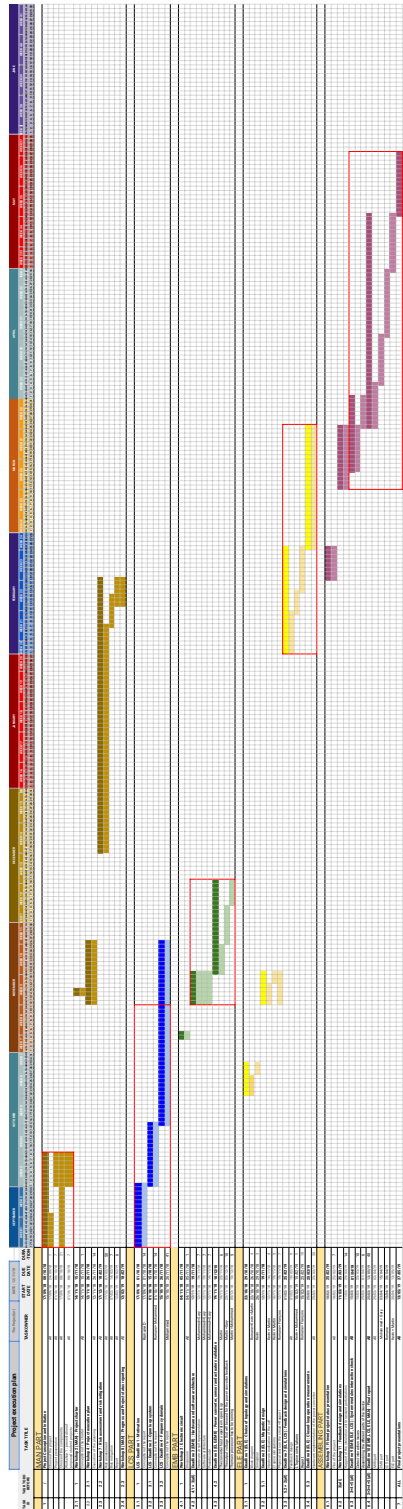


Figure 63: Project execution planning.

9.2 Risk management

DESIGN FAILURE MODE AND EFFECTS ANALYSIS Analog									
Failure Mode / Failure Cause		Failure Effects		Current Controls		Recommended Actions		Responsible Team	
No.	Root Cause / Safety / Part	Failure Mode / Failure Cause	Failure Effects	Control / Prevention	Severity before	Action required	Target Completion Date	Team	Action review date
Normal / Safety / Part									
Block - 1	Power Function Requirements	Potential failure mode 1 External effects of values Input signal to the high voltage converter not functioning properly, difficulty of assembly code	Microcontroller doesn't have appropriate signal at the back, bad connection or a bad insulation	Measure the output voltage after connection	4	As planned	17/11/2018	R&D	10/12/2018
Block - 3	Having a efficiency of above 90%	Having a efficiency below 90%	Bad design in the circuit	Measure the efficiency after connection	18			Team	
Block - 4	Constant output voltage	Causes damages our electronic circuit	Bad design in the circuit	Measure the output voltage after connection	2			Team	
H Bridge - 1	Deliver good control signal for the DC motor	Oscillations during the motor rotation and the noisy signal	Motor in the circuit	Check the quality of the component and make a good connection	2			Team	
DC motor - 1	Motor which runs depending on the heat	Detector	This motor doesn't turn, doesn't work correctly	Washing the motor and cleaning system is working	2			Team	
LARM08 - 1	Constant output voltage	Overheated at the later of the power up	Burn the microcontroller, and sensors	Reusing the element	2			Team	
LARM09 - 2	Reduce the voltage to 24V to supply the output voltage not by	Burn the microcontroller, and sensors	Bad choice of the component or noise	Test the component before using it	2			Team	
Angular sensor - 1	Good range measurement	Leds a blurry tracking	Bad resolution or bad choice of the component	Test the resolution of the sensor	12			Team	
Ultrasonic sensors - 1	Provide distance to first object encountered	Increased thermal noise to a microcontroller related to the detection of the floor. Not for running a fast tracking	Angle is detected too large	Check the angle of the component	1			Team	
Ultrasonic sensors - 2	Provide distance to first object encountered	Error in the static error of the distance	Bad accuracy of the sensor	Check the distance of the component	13			Team	
Control system - 1	Situations are good in practice	Not representative of the reality	Bad reference tracking, unstable system	Simulations in simulation software	2			Team	
Microcontroller PIC - 1	LCR implementation works fine	detective PIC board coding	Bad tracking no tracking at all	Check the difference between the simulation and the real tracking	10			Team	
Microcontroller PIC - 2	Monitor the block controller	Bad monitoring of the block	No stop signal to our circuit	Test the component	7			Team	
Microcontroller PIC - 3	Control the system	Not around immunity in the microcontroller	Can't implement control system in the microcontroller	Check the immunity in the microcontroller	48			Team	
230V to 240V converter - 1	Convert 230V AC to 240V DC (230V Sector)	Block converter is not correctly supplied from the sector	Block down the work (well)	Ask a technician	3			Team	
230V to 240V converter - 2	Convert 230V AC to 240V DC (230V Sector)	Block converter is not correctly supplied DC output voltage too high	Block down the work (well)	Measure the output voltage	14			Team	
230V to 240V converter - 3	Convert 230V AC to 240V DC (230V Sector)	Block converter is not correctly supplied DC output voltage too low	Block down the work (well)	Measure the output voltage	14			Team	

Figure 64: Risk management FMEA.

9.3 Linear control systems part : Gang of "2"

Now the closed-loop system is designed we have to check if the system described by its closed-loop transfer function $L(s)$ is well designed thanks to the implemented controller. This analysis is done by interpreting 2 functions : the sensitivity function $S(s)$ and the complementary one $T(s)$ which depend on $L(s)$, $C(s)$ and $P(s)$.

These functions will thus illustrate if the noise is well rejected, if the reference tracking is well performed by the motor and if this tracking is impacted by changes in the disturbance or not. These effects will be analyzed on both the controllable input and the system output, at low and high frequencies.

Sensitivity function S(s)

The sensitivity function depends on the closed-loop transfer function $L(s)$ and is defined as follows :

$$S(s) = \frac{1}{1 + L(s)}$$

A trade-off has to be made because $|S(s)| \rightarrow 1$ if we want our output to reject noise but $|S(s)| \rightarrow 0$ to have an output which is not affected by disturbances. We will thus respect one condition at low frequencies and the other one at high frequencies.

In practice for a good design we have :

$$d \rightarrow y : |S(s)| \simeq 0 \text{ at low frequencies}$$

$$n \rightarrow y : |S(s)| \simeq 1 \text{ at high frequencies}$$

because we want the output y to be reactive to the disturbances around the work frequency, so at low frequencies, while we want to reject as much noise as possible at high frequencies.

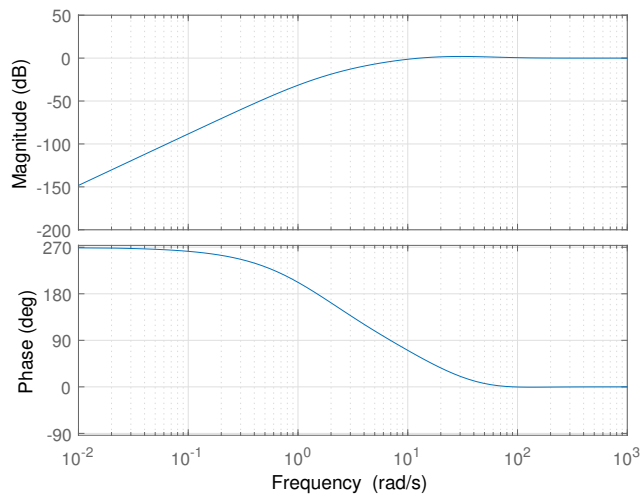


Figure 65: Sensitivity function bode diagram.

Figure 65 shows the bode diagram of the sensitivity function. In this last one we can see that at low frequencies the magnitude tends to minus infinity in logarithm scale. This corresponds thus to 0 in natural units and thus the condition at low frequencies is well fulfilled. The disturbance does not really affect the output of the system. At high frequencies the magnitude bode diagrams tends to 0dB. This value corresponds thus to 1 in natural units and the condition

for the noise is thus well respected. The system output is not affected by the noise at high frequencies.

Let us note that the peak when the magnitude reaches 1dB is related to the robustness of our system.

Complementary sensitivity function $T(s)$

The complementary sensitivity function depends on the closed-loop transfer function $L(s)$ and is defined as follows :

$$T(s) = \frac{L(s)}{1 + L(s)}$$

Again a trade-off has to be done for $|T(s)|$: $T(s) \rightarrow 1$ for a good reference tracking but $|T(s)| \rightarrow 0$ to have an input which is not affected by the noise.

In practice, for a good design we have :

$$r \rightarrow y, u : |T(s)| \simeq 1 \text{ at low frequencies}$$

$$d \rightarrow u : |T(s)| \simeq 1 \text{ at low frequencies}$$

$$n \rightarrow u : |T(s)| \simeq 0 \text{ at high frequencies}$$

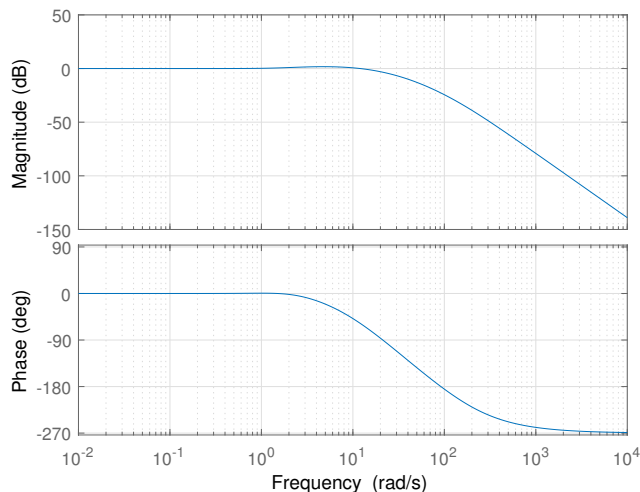


Figure 66: Complementary sensitivity function bode diagram.

Figure 66 represents the bode diagram of complementary sensitivity function. This last one show that at low frequencies the magnitude is equal to 0dB. This value corresponds thus to 1 in natural units and the conditions wanted in practice are thus fulfilled. In fact when the amplitude tends to 1 the disturbance does not affect the input the the reference is well tracked, this for both the input and the output of the system. At high frequencies the magnitude tends to minus infinity. This corresponds thus to 0 in natural units and thus the system is well designed at high frequencies. Indeed we wanted the input to reject the noise at high frequencies and the condition for that defined previously was that the amplitude tends to 0.

Conclusion

The gang of "2" analysis has shown that the controller and thus the closed-loop system are well design. Both the input and the output fulfill the expected conditions : the system tracks well the reference, this one is not affected by the changed in the disturbance and reject the noise at high frequencies.

Let us note that the 2 others functions of the gang of 4 have not been analyzed in this section. The reason is that these depend on $S(s)$ which has been analyzed and thanks to which we have concluded that the system was well designed. Also The behaviour of both the input and the output have been analyzed thanks to $S(s)$ and $T(s)$ only.

References

- [1] Lucien Bachelard. Hc-sr04 - module de détection aux ultrasons - utilisation avec picaxe, Nov 28, 2015. URL: <https://www.gotronic.fr/pj2-hc-sr04-utilisation-avec-picaxe-1343.pdf>.
- [2] Bernard Boigelot. Embedded systems, 2018. URL: <http://www.montefiore.ulg.ac.be/~Boigelot/cours/embedded/index.html>.
- [3] Fabrice Frebel. Elements of power electronics, 2018. URL: <http://www.montefiore.ulg.ac.be/~frebel/ELEC0055/Schedule.html>.
- [4] Microchip. 28-pin 8-bit advanced analog flash microcontroller (pic16f1788/9 data-sheet), 2013 - 2015. URL: <http://ww1.microchip.com/downloads/en/DeviceDoc/40001675C.pdf>.